DISSERTATIONS IN
FORESTRY AND
NATURAL SCIENCES

Arto Koistinen

Improvement of Orthopaedic Bone Screws by DLC Coatings

In Vitro Methods for Testing of Screw Fixation

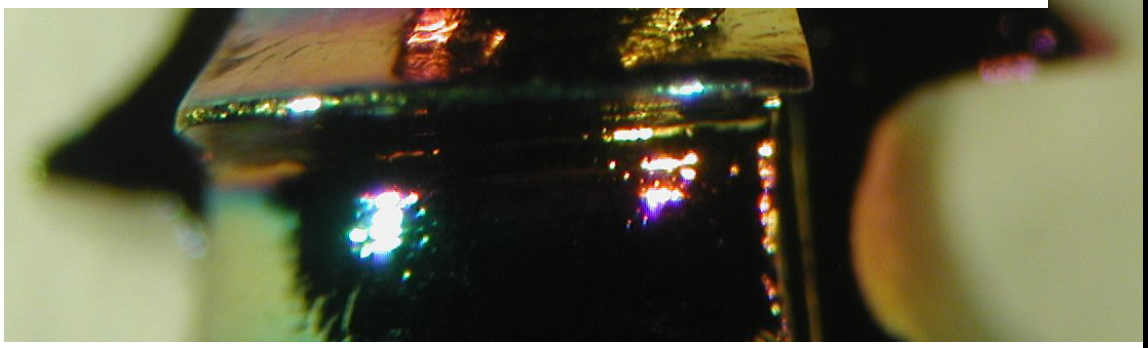

Publications of the University of Eastern Finland
Dissertations in Forestry and Natural Sciences

UNIVERSITY OF
EASTERN FINLAND

ARTO KOISTINEN

Improvement of Orthopaedic Bone Screws by DLC Coatings

In Vitro Methods for Testing of Screw Fixation

Publications of the University of Eastern Finland
Dissertations in Forestry and Natural Sciences
No 89

Academic Dissertation
To be presented by permission of the Faculty of Science and Forestry for public examination in the Auditorium L22 in Snellmania Building at the University of Eastern Finland, Kuopio Campus, on 30th November, 2012, at 12 o'clock noon.

Department of Applied Physics

Kopijyvä Oy
Kuopio, 2012
Editors: Prof. Pertti Pasanen, Prof. Pekka Kilpelinen,
Prof. Kai Peiponen, Prof. Matti Vornanen

Distribution:
University of Eastern Finland Library / Sales of publications
P.O. Box 107, FI-80101 Joensuu, Finland
tel. +358 294 45 8145
julkaisumyynti@uef.fi
http://www.uef.fi/kirjasto

ISBN: 978-952-61-0961-9 (printed)
ISSNL: 1798-5668
ISSN: 1798-5668
ISBN: 978-952-61-0962-6 (pdf)
ISSN: 1798-5676

Author's address:
University of Eastern Finland
Department of Applied Physics
SIB-labs, Kuopio Campus
P.O.Box 1627
70211 KUOPIO
FINLAND
email: arto.koistinen@uef.fi

Supervisors:
Professor Reijo Lappalainen, Ph.D.
University of Eastern Finland
Department of Applied Physics
P.O.Box 1627
70211 KUOPIO
FINLAND
email: reijo.lappalainen@uef.fi

Professor Heikki Kröger, M.D., Ph.D.
Kuopio University Hospital
Department of Orthopaedics, Traumatology
and Handsurgery
P.O.Box 1777
70211 KUOPIO
FINLAND
email: heikki.kroger@kuh.fi

Reviewers:
Professor Michiaki Takagi, M.D., Ph.D.
Yamagata University
Department of Orthopaedic Surgery
2-2-2 Iida Nishi
Yamagata 990-9585
JAPAN
email: mtakagi@med.id.yamagata-u.ac.jp

Centre Manager Lars Pleth Nielsen, Ph.D., M.Sc.
Danish Technological Institute
Tribology Centre
Kongsvang Allé 29
8000 Århus C
DENMARK
email: lars.pleth.nielsen@teknologisk.dk

Opponent:
Professor Carina B. Johansson, Ph.D.
University of Gothenburg
The Sahlrenska Academy
Department of Prosthodontics
P.O.Box 450
405 30 Göteborg
SWEDEN
email: carina.johansson@odontologi.gu.se

ABSTRACT

Bone screws are the most common implants in orthopaedics and dentistry. Common causes for failure of bone fixation are poor bone quality and infection that cause inadequate bone–screw interface stability, leading to loosening of the fixation device. Thus, numerous stabilizers (*i.e.* the screws and plates) are removed in a secondary operation. Especially, corroded surfaces can complicate removal of the screws and lead to failure of a screw or bone.

Diamond-like carbon (DLC) coating, produced by physical vapour deposition techniques, is proven to have outstanding tribological properties and is tolerated well by the human body. High-quality DLC coating (*i.e.* coatings with high amount of sp^3 diamond bonds) can be considered to be biocompatible according to *in vivo* and *in vitro* experiments. In this thesis, performance of DLC coating on fracture fixation screws was studied with *in vitro* mechanical tests. A customized test equipment was developed for testing of bone screws. Specifically, screw insertional torque and pull-out strength, frictional properties of the coating and mechanical properties of the test materials have been studied in the thesis.

DLC coating resulted in at maximum 50 % lower insertion torque compared with uncoated screws in the cortex of human cadaver bone. In standard materials modeling bone, 10–15 % improvement in insertion torque was found. Pull-out strength of the screws and coefficient of friction was not significantly affected by DLC coating. Fixation strength of the screws is clearly dependent on the mechanical properties of the test blocks, such as bone mineral density or elastic modulus of the material. Thus, the proper choice of materials is also relevant for valid *in vitro* testing.

Novel coatings provide exceptional interfacial properties (such as hardness, smoothness and inertness) improving *e.g.* bone-implant interaction or tribology. *In vivo* tests are eventually required to approve the DLC coatings in long-term physiological use. However, also *in vitro* testing is needed for initial testing of hypotheses, but one should also consider proper test materials and type of biomechanical tests for each application.

National Library of Medicine Classification: QT 36, QT 37, WE 185

Medical Subject Headings: Biomedical and Dental Materials; Coated Materials, Biocompatible; Diamond; Bone Screws; Materials Testing; in vitro

Yleinen suomalainen asiasanasto: biomateriaalit; pinnoitus; timantti; luuruuvit; aineenkoestus; in vitro -menetelmä

To Erika, Ronja, Mona, Peetu and Iisa

Acknowledgements

This study was carried out in the Department of Applied Physics and in SIB-labs, University of Eastern Finland and also formerly in BioMater Centre, University of Kuopio.

Firstly, I want to thank my first supervisor Professor Reijo Lappalainen, Ph.D. for his guidance during the thesis. His enthusiasm and knowledge in the field of coatings have been the thrust for this study. I also owe thanks to the advisory supervisor Professor Heikki Kröger, M.D., Ph.D. as well as to late Professor Seppo S. Santavirta, M.D., Ph.D. (who passed away in 2005) for their clinically relevant advises and really positive spirit.

I want to express gratitude to the Reviewers Professor Michiaki Takagi, M.D., Ph.D. and Centre Manager Lars Pleth Nielsen, Ph.D., M.Sc. for their constructive criticism and suggestions for improving the thesis.

Special thanks belong to Prof. Lappalainen's research group and especially following persons: Hannu Korhonen, M.Sc. (Tech.), Jari Leskinen, M.Sc. and Mikko Selenius, M.Sc. The study and work would not have been possible without your help as well as long-lasting friendship and 'fruitful' co-operation. Also, the chief laboratory technicians Ritva Sormunen, Virpi Miettinen and Juhani Hakala are greatly thanked for their help and understanding in my work as a researcher and supervisor.

Finally, I wish to thank my beloved family Erika, Ronja, Mona, Peetu and Iisa, who have been the greatest joy and at the same time the greatest challenge in my life during the latest years. Also I am grateful to my parents Elina and Timo, and to my sister Anu for the encouraging environment during my childhood and youth. My mother would have been proud to see her son in the dissertation.

Following institutions and foundations are gratefully acknowledged for financial support during this project: The National Technology Agency (TEKES), Finland; the National Doctoral Programme

of Musculoskeletal Disorders and Biomaterials, Finland; BioMater Centre, University of Kuopio, Finland; Finnish Cultural Foundation of Northern Savo, Kuopio, Finland; Science Foundation of Instrumentarium Corporation, Helsinki, Finland; Finnish Academy of Science and Letters, Vilho, Yrjö and Kalle Väisälä Foundation, Helsinki, Finland; The Scandinavia-Japan Sasakawa Foundation, Helsinki, Finland; Emil Aaltonen Foundation, Tampere, Finland.

Kuopio, November 2012

Arto Koistinen

LIST OF PUBLICATIONS

This thesis is based on the following original articles, which are referred to by the Roman numerals I - IV:

I Koistinen A., Santavirta S.S. and Lappalainen R., "Apparatus to test insertion and removal torque of bone screws", *Proc. Inst. Mech. Eng. H* **217**: 503–508 (2003).

II Koistinen A., Santavirta S.S., Kröger H. and Lappalainen R., "Effect of bone mineral density and amorphous diamond coatings on insertion torque of bone screws", *Biomaterials* **26**, 5687–5694 (2005).

III Koistinen A.P., Korhonen H., Kiviranta I., Kröger H. and Lappalainen R., "Analysis of plastic deformation in cortical bone after insertion of coated and non-coated self-tapping orthopaedic screws", *Proc. Inst. Mech. Eng. H* **225**, 629–639 (2011).

IV Koistinen A.P., Korhonen H., Kröger H. and Lappalainen R., "Interfacial sliding properties of bone screw materials and their effect on screw fixation strength", *submitted for publication in J Appl Biomater Function Mater*.

AUTHOR'S CONTRIBUTION

The publications selected in this dissertation are original research papers on biomechanical *in vitro* testing of novel amorphous diamond (AD) coatings on medical applications. The original idea of the present studies was originated from the clinical problem arose by prof. Seppo Santavirta and solution suggested by prof. Reijo Lappalainen.

Testing protocols and equipment were designed in co-operation by the author and Prof. Lappalainen in paper **I**. The author is responsible for conducting all tests and analysis of the data. In papers **II** and **III** the author is responsible for all biomechanical testing, imaging and data analysis, except for μCT imaging. The idea for paper **IV** came from the author. The author is also responsible for data analysis and biomechanical tests, except for frictional tests.

The author has written all the manuscript to the papers **I–IV** with the co-operation of the co-authors.

LIST OF ABBREVIATIONS AND SYMBOLS

AD	amorphous diamond
AISI316L	a ”surgical grade” of stainless steel
CVD	chemical vapour deposition
DLC	diamond-like carbon
FPAD	filtered pulsed arc discharge; a PVD coating method
in vivo	within a living organism
in vitro	in an artificial environment outside the living organism
LA	laser ablation; a PVD coating method
PMMA	polymethyl-metacrylate
POM	polyacetal
PTFE	polytetrafluoroethylene
pQCT	peripheral quantitative computed tomography
PVD	physical vapour deposition
SEM	scanning electron microscope
SS	stainless steel
USPLD	ultra-short pulsed laser deposition; a PVD coating method
μCT	micro-computed tomography
BMD	bone mineral density
CBA	cortical bone area
CoF	coefficient of friction
$CSAC$	cross-sectional cortical bone area
I_{pol}	polar moment of inertia
N	number of samples
p	significance level
R	correlation coefficient
ThC	cortical thickness
τ	torque
μ	coefficient of friction, CoF

Contents

1 Introduction and objectives

Different types of bone screws and implants are used in orthopaedics for treatment of bone fractures. In fracture fixation, the main objective is maintaining the stability of the fracture site. Therefore, fracture fixation devices must secure geometric alignment, transmit compressive forces with minimum motion across the fracture site, and avoid excessive tensile or shear stresses across it. On the other hand, the fixation device should allow favorable mechanical and biological conditions for healing [1,2].

Common causes for failure of the fixation are poor bone quality and infection that cause inadequate bone-screw interface, leading to loosening of the fixation device. On the other hand, corroded surfaces can complicate late removal of bone screws and lead to failure of a screw or bone [3–7]. Also biological factors including the properties of the bone, such as the thickness of cortices and the density of bone, influence the implant survival as well as the forces required in screw installation, removal or pull-out [4,5,8–14].

Improvement of osseointegration has been widely studied as a potential solution to the problem of creating a higher stability of implants. Titanium-based coatings and hydroxyapatite coatings are the most common solution in this context [15–17]. However, not all fracture fixation devices are intended for long-term *in situ* use in the body. Most fractures heal in a reasonably short time and the stabilizers (*i.e.* the screws and plates) can be removed in a secondary operation to avoid *e.g.* stress–shielding effects.

On the other hand, coatings can prevent bacterial adhesion, decrease friction or minimize wear on sliding surfaces [18,19]. Diamond-like carbon (DLC) has outstanding tribology properties and is, additionally, not rejected by the body [19–21]. Thus, the use of DLC

coatings could lead to fewer screw failures and lower torque levels during insertion and removal, *i.e.* reduced energy absorption of the bone and less bone damage.

The hypothesis of this study was whether bone screw fixation can be improved by using high-quality DLC coatings. The hypothesis was firstly studied by constructing and validating a custom-made equipment for testing of screw insertion and removal properties *in vitro* using synthetic and natural test materials. Thereafter, the equipment was used to install non-coated and DLC–coated screws into human cadaver bones to study screw insertion and removal characteristics. The bone deformation due to screw insertion was analyzed in detail using various microscopic techniques after screw removal and sample preparation. Finally, knowledge on factors affecting screws' interfacial sliding mechanisms was increased by studying also friction and pull-out strength of the screws.

Story behind the present study: Screw failure during a revision surgery causes additional damage to the tissues due to effort needed to remove the failed pieces of screws. This leads to prolonged healing time as well as increased operation time. The above described problem is observed by surgeons throughout the clinics and was brought up by late professor Seppo Santavirta. Thus, development of screws (especially long and thin cortical screws) by enhancing their surface properties with the aim of easing late removal would be appreciated. As a solution, novel DLC coatings with high biocompatibility and hardness but with low wear rate was introduced by professor Reijo Lappalainen. This was selected as the main topic of the thesis and studied by the author.

2 Bone

2.1 BONE COMPOSITION

Bone is a composite tissue consisting of mineral, matrix, cells, and water. Bone consists mostly of the mineral calcium hydroxyapatite [$Ca_{10}(PO_4)_6(OH)_2$], collagen and glycosaminoglycans which bind collagen. Hydroxyapatite is strong in compression, whereas collagen gives flexibility and tensile strength. The mineral is an analog of the naturally occurring crystalline calcium phosphate, hydroxyapatite. Physiologic mineral crystals, as distinct from geologic apatites, are very small and imperfect, containing fewer hydroxyl groups and many impurities such as carbonate, fluoride, acid phosphate, magnesium, and citrate.

The bone matrix is essentially type I collagen. The collagen fibrils are arranged in the extracellular matrix in patterns related to the function of the tissue in which they are found. The unique triple helical structure of collagen provides strength and flexibility to most of the connective tissues [22]. The mineral crystals add extra rigidity to the collagen fibers. Collagen is stabilized by cross-links formed post-translationally in the extracellular matrix. The nature of these cross-links differs in the mineralized and non-mineralized connective tissues [23]. Analyses of the cross-links that stabilize bone collagen, as opposed to skin and tendon collagen, provide a useful marker for diseases such as osteoporosis in which breakdown of the matrix is increased [24]. In addition to collagen, about 5% of the extracellular matrix of bone is made up of noncollagenous proteins. These proteins play crucial roles in mineral homeostasis, bone metabolism, bone formation, and bone turnover [25, 26]. Distributions of mineral and matrix proteins differ in various bones, and these also change with disease and age.

2.2 BONE STRUCTURE AND FUNCTION

2.2.1 Bone cells

Bone provides skeletal support and protection for the soft tissues and a centre for mineral metabolism [27]. Bone serves as source for calcium, magnesium, and phosphate ions as well as the mineral crystals in bone provide strength and rigidity to the matrix upon which they are deposited. Furthermore, another major function of bone is mechanical, *i.e.* facilitating mobility with muscles.

The metabolism, formation, and turnover of bone is governed by cells. Bone has three cell types: osteoblasts, osteocytes, and osteoclasts. Osteoblasts and osteocytes are derived from the mesenchymal cell lineage and appear to be closely related. Osteoblasts synthesize and secrete the bone matrix. Osteocytes are enmeshed in an existing bone matrix and appear to be more important in conveying nutrition and information throughout bone. In contrast, osteoclasts are multinucleated giant cells and they are believed to be of macrophage origin. They are the cells responsible to resorbing bone. Osteoprogenitor cells are an additional cell type that line Haversian canals and periosteum prior to differentiation into other cells.

In normal tissues, the functions of osteoblasts and osteoclasts are coupled such that signals from one affect the other [28]. The distribution of these bone cells and their relative activities vary with type of bone, age, and disease state.

2.2.2 Bone types

Different development phases of bone tissue exist in human body; mature (lamellar) and immature (woven) bone. Lamellar bone is organized, regular, stress-orientated, and can be cortical or cancellous bone. Woven bone has high cell turnover and content, less orientated structure and higher water content. Both consist of cells, and partly organic, partly mineral extracellular matrix of collagen fibres [27].

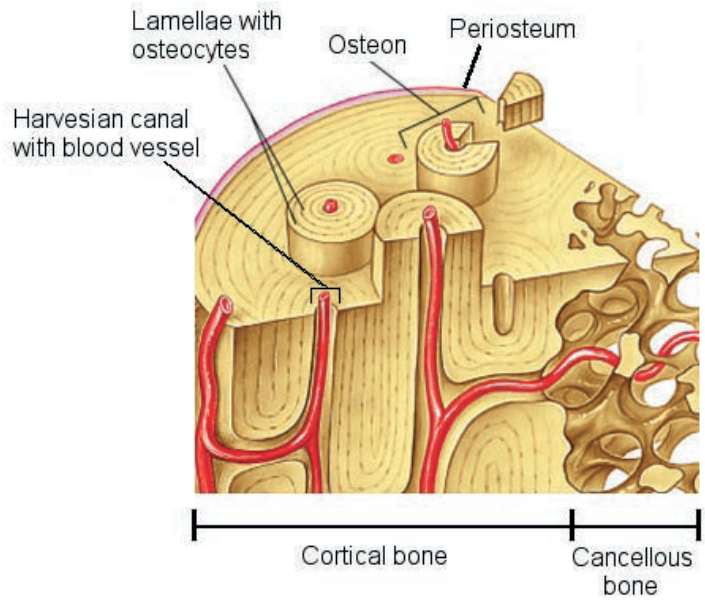

Figure 2.1: Schematic illustration of bone structure. (Modified from [29].)

To describe the structure of lamellar bone in detail; *Cortical bone* consists of tightly packed Haversian systems (osteons) with central Haversian canal for nerves and vessels (see Figs. 2.1 and 2.2). Turnover in cortical bone is slow and occurs at the Haversian canals and osteons. In contrast, *cancellous bone* has faster turnover and its structure is less dense. Only 20 % of weight of the skeleton is cancellous [27].

Periosteum is a dense layer of fibro-connective tissue surrounding bone. Inner layer of periosteum is vascular and osteogenic, while outer layer is fibrous and continuous. Periosteum plays an important role in fracture healing.

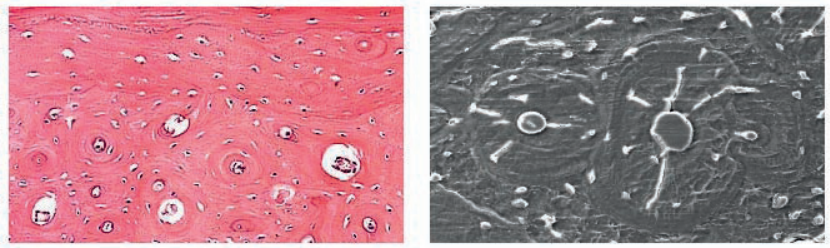

Figure 2.2: Cortical bone imaged by optical (left) and scanning electron microscopy (right). The images show *e.g.* round osteons with Haversian canal in the middle.

2.3 BIOMECHANICS OF BONE

The primary responsibility of the skeleton is to provide structural support for the body. In this role, the skeleton is the basis of posture, opposes muscular contraction resulting in motion, withstands functional load bearing, and protects internal organs.
Organic component consists type I collagen for tensile strength, proteoglycans for compressive strength, glycoproteins and phospholipids. Tensile strength is increased by cross-linking. Forty percent of the matrix is organic, from which 90% is collagen.
Inorganic component consists minerals, mostly poorly crystalline calcium hydroxyapatite, which mineralizes bone and provides compressive strength.

The weakest area in bone is the cement line between osteons. Bone is 3 times as light, 10 times as flexible but has approximately the same tensile strength as cast iron.

Parameters that describe materials' mechanical properties are *e.g.* stress, strain, (stress-strain curve), yield point, modulus of elasticity and ultimate strength (see Fig. 2.3). These parameters are described in detail in the following.

Strain When a force is applied to any material, such as bone, it

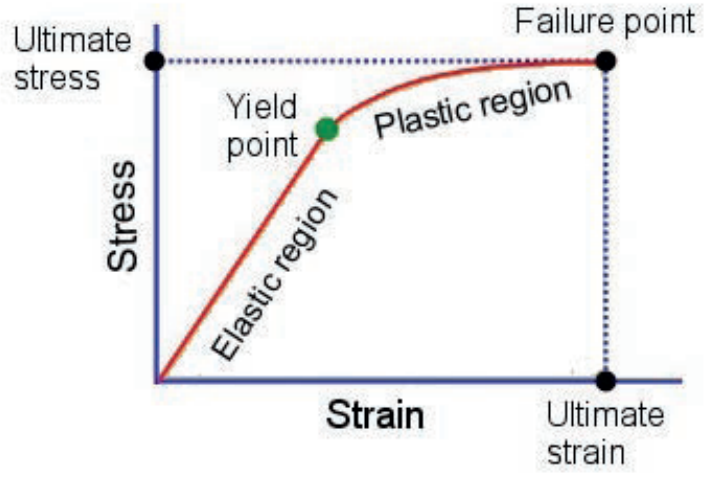

Figure 2.3: Fundamentals of bone's stress - strain curve under compressive loading.

deforms. Strain is defined as the change in length (*i.e.* deformation) divided by its original length ($\tau = \Delta L/L$). When a material is pulled, it gets longer (tensile strain) and when pushed together, the material shortens (compressive strain). Shear strain arises when layers of material slide against another, as might occur with torsion or bending [30]. The yield compressive strain of cortical bone is in the order of 0.5 % [31].

Stress The force per unit area is the stress ($\sigma, = F/A$), and is reported in pascals (Pa). This parameter aids in comparing specific test with other materials, and it is preferable to report the magnitude of the force in terms of the cross-sectional area of the material on which it is acting [32].

Elastic modulus The degree to which a material deforms depends not only on the magnitude of the forces and moments (turning, twisting or rotation), but also on the stiffness of the constituent materials [33]. During the initial stage of a test to define material properties, there is a linear increase in strain

as the stress increases. This is known as the elastic region (see Fig. 2.3). Should the load be removed during this phase of the test, the specimen will return to its original size and shape, without permanent damage. The linear relation between strain and stress is called Hooke's Law ($E = \sigma/\tau$; where E is the elastic modulus). Ut tensio, sic vis: as the extension, so the force [34]. Thus, the slope of the elastic region of the stress-strain curve reflects the stiffness of the material, otherwise known as the *modulus of elasticity*.

In the case of bone, stiffness is determined by the relative proportions of the hydroxyapatite crystals and the collagen fibers that make up the composite [35]. A material, such as bone, that has distinct mechanical properties in different directions is *anisotropic*. The modulus of mature cortical bone is on the order of 18 GPa in the longitudinal direction, 12 GPa in the transverse direction, and 3.3 GPa in shear [36]. The material properties of cancellous bone are even more complex, as trabecular orientation, connectivity, and density greatly influence the stiffness [37]. Depending on location, the modulus of trabecular bone can range from 0.1 to 3.5 GPa [38]. The degree of mineralization (*e.g.*, immature or woven bone) or porosity (*e.g.*, old bone) will compromise the stiffness of the bone and thereby lower the elastic modulus.

Yield stress When the increase in strain is no longer linearly proportional to the stress, the elastic region of the deformation ends. At the same time material looses its ability to resume the original shape (yield point in Fig. 2.3). The specimen has moved into the plastic region where permanent damage has begun to occur. In terms of bone, yield failure arises through ultrastructural microcracks within the hydroxyapatite and the disruption of the collagen fibrils. For cortical bone, the yield compressive stress is approximately 130 MPa [31].

Ultimate stress As loading continues in the plastic region, the material will eventually reach ultimate failure point, at which the

specimen fails catastrophically. The point at which the bone breaks can be viewed as either the ultimate strain or the ultimate stress (140 MPa in tension, 200 MPa in compression, and 65 MPa in shear) [39]. Because of this disparity, it should become clear that the cause of fracture in ”normal” bone material is most likely due to tensile or shear failure.

The amount of postyield strain that occurs before ultimate failure is a measure of the material's *ductility*, reflecting its ability to resist the propagation of cracks [32]. A ductile material is one that can change form without breaking; a tendon is more ductile than bone. A material that manages little postyield behavior before ultimate failure is considered brittle (*e.g.*, glass or ceramic).

Toughness The stress-strain curve yields another important property of the material. The area under the curve reflects the amount of work (or energy per unit volume) possessed by the material at any given point on the curve. At ultimate failure, the area under the curve defines the energy required to break the object, or *toughness*. A major contributor to the toughness of bone is its composite nature of haversian, circumferential, and interstitial lamellae.

Bone, as an organ, has a requirement to be both stiff and tough. These two attributes must be attained by a balance between the resistance to crack propagation provided by collagen and the resistance to deformation provided by the mineral. Comparatively small changes in the mineral content of bone tissue can have significant effects on its properties as a material [40].

Areal properties of bone Areal properties define the overall mass and pattern of the bone structure. They are also important to the ultimate success of the skeleton. Size, density or architecture describe areal properties at the gross level. However, also other areal properties are key contributors to the structural performance of bone, including the long-bone curvature, ge-

ometry of the cross-sectional area, or the trabecular organization.

Even the simplest of loading create complex strain and stress environments in bone. Axial loads applied will cause tensile strain on the convex side, and compressive strain on the concave side of the bone. The flexural rigidity, EI, represents the amount of force per unit cross-sectional area required to deform the material, where E is elastic modulus, and I is the moment of inertia of the material [41]. The moment of inertia reflects the contribution of each bit of material to the stiffness in each position in the cross-section ($I = ly^2dA$, where y is the distance of each element of area A from the neutral axis along the length l).

2.3.1 Bone as a composite

Bone must operate in a complex environment which necessitates high demands for the structure, composition and function of the bone. The composite structure of bone allows it to withstand compressive and tensile stresses, as well as bending and torsional moments. The inorganic phase of bone, with hydroxyapatite crystals arrayed in a protein matrix, provides the ability to resist compression. Individual calcium phosphate crystals of multiple sizes are imbedded in and around the fibrils of the collagen type I lattice [42]. Hydroxyapatite crystals, although effectively resisting compressive loads, have a poor ability to withstand tensile loads. In the case of bone, this tensile strength arises from collagen fibrils organized into lamellae.

Whereas the ultrastructural organization is defined by the genome, the functional environment also contributes to the distribution of lamellae as well to the osteons that house them [43]. This directed deposition of collagen adds to the anisotropy of the bone. Given that $> 80\%$ of functional strains are due to bending (and thus a high percentage of strain is tensile), the structural quality of the bone may ultimately be determined by the quality of the collagen

and the organization of the microarchitecture. Recent studies have shown that collagen itself deteriorates with age and contributes to the declining material properties of the skeleton [44]. Alterations in either the organic (*e.g.*, collagen) or inorganic (*e.g.*, hydroxyapatite) matrix components can bring about changes in bone strength.

Bone is sensitive to its mechanical environment, and to a large extent, it is this functional environmant that defines skeletal structure and ultrastructural organization. This ”form follows function” aspect of skeletal tissue is known as Wolff’s Law and helps us to understand how exercise serves as an anabolic agent to bone, and how disuse, cast immobilization, and bed rest put the skeleton at risk [45].

Wolff’s law Julius Wolff published his seminal 1892 work on bone remodeling, or the observation that bone changes its shape in response to stress acting on it. ”Wolff’s law” states that bone remodels in response to the mechanical stresses it experiences so as to produce an anatomical structure best able to resist the applied stress.

2.4 BONE FRACTURE

Despite bone’s capacity to withstand great forces and ability to change its structure according to functional environment, bone failures also occur at extreme conditions.

Typical fracture patterns depend on direction of loading; tension - transverse, compression - oblique, bending - tension side first and then compression side $\rightarrow$ butterfly, torsion - spiral fragment. For a fatigue fracture, the rate of microfracture exceeds the rate of repair. The reasons are (a) stress fracture follows fatigue from repetitive stress, or (b) there is defective muscle activity and absence of protective muscle function predisposes to fracture.

Fractures occur at the ultimate strength, and they are affected by patient–related (intrinsic) and extrinsic factors [27].

Intrinsic factors include:

- Bone density: Compressive and tensile strength of bone is proportional to the density. Porosity of cortical bone is 3-30 %, whereas cancellous bone can have porosity of over 90 %. Cancellous bone is 10 % as stiff, but 500 % ductile as cortical bone.
- Patient age: Modulus of elasticity reduces by 1.5 % *per annum*, and ultimate strength reduces by 5-7 % per decade after reaching maximum values around 30 years of age.
- Bone geometry: The larger cross-sectional area, the greater the stress to failure. The longer the bone, the greater the potential bending moment.
- Wolff's law: Bone is formed in response to stress and resorbed where stress is absent.
- Stress raisers: A cortical defect occupying 20 % of the diameter can reduce the strength of the bone by up to 60 %. (Note: For example screw defects heal in normal bone in 8 weeks.)
- Muscle function: Muscles protect the bone.

Extrinsic factors include:

- Magnitude of the force: The stiffer the bone, the more energy will be released at the time of fracture.
- Rate of stress: Bone is *viscoelastic* - the ultimate strength increases when loaded at faster rate.
- Direction of stress: Bone is anisotropic - properties differ when loaded in different directions. Bone is strongest in compression, weakest in tension, and intermediate in shear.
- Fatigue failure: Bone fails at lower stresses when stressed repeatedly. Bone's natural ability to repair microfractures protects from this phenomenon.

2.5 BONE HEALING AND GROWTH

Healing of bone fracture is a specialized form of tissue healing. The periosteum plays a vital role in fracture healing. In practice, fracture healing process is similar to the process occurring at an active growing plate; Woven bone formed within callus after a fracture is replaced by lamellar bone. Rigid internal fixation interferes with natural process, leading to direct or primary healing without abundant callus formation [27].

Healing consists three phases: acute inflammation, repair and remodelling. Short definitions of the phases is as follows:
Acute inflammation - First phase of healing in response to haematoma formation at the fracture site. Haematoma provides cells secreting growth factors (cytokines) to promote healing.
Repair process - Repair starts with organization of the haematoma into granulation tissue and promoting alkaline phosphatase activity. Osteoclasts resorb the non-viable bone. Proliferation of mesenchymal stem cells leads to formation of a matrix of fibrous tissue and cartilage. After mineralization woven bone, described as fracture callus, is formed. When the fracture margins are stable and anatomically aligned (probably due to rigid internal fixation), direct bone healing occurs. Initial healing occurs without abundant fracture callus formation and replacement, similarly to remodelling or natural turnover of bone. Defect up to 200 micrometer can be crossed by this manner, known as contact healing. Larger gaps are first filled with woven bone and then lamellar bone before remodelling [27].
Remodelling phase - Remodelling starts during the repair phase and consists the conversation of woven bone to lamellar bone. The process may take several months or years. The bone returns to its normal shape by responding to loading and stress, *i.e.* Wolff's law [27].

Injury variables affecting bone healing include soft tissue damage or interposition, infection, bone disease and poor local blood

supply. Patient variables include age, smoking, malnutrition, corticosteroids. Fracture healing is also altered by the presence or absence of surgical stabilizers, such as screws or pins.

After initial healing and new bone formation, it remains in a dynamic state. Bone remodels constantly with the aim to provide maximum strength with minimum mass (Wolff's law), to allow growth, and to provide a source of mineral ion homeostasis. The remodeling processes (formation and resorption) are linked so that factors produced by bone-forming cells (osteoblasts) activate remodeling cells (osteoclasts) and vice versa [34].

Basic phenomena and their characteristics of bone growth include [27];

Osteogenesis *i.e.* bone formed on fibrous tissue. Occurs during embryonic development, early stages of growth, and during healing. Two major subclassifications: intramembranous ossification and endochondral ossification (intramembranous - bone formed on soft fibrous tissue; endochondral - bone formed on cartilage). Large amounts of bone can be produced when necessary.

Modelling *i.e.* bone formed on existing bone tissue. Occurs during growth and healing; Osteoblasts and osteoclasts act independently at different sites. Large amounts of bone can be created or resorbed when necessary.

Remodelling , *i.e.* bone both resorbed and formed at the same site. Occurs from growth through death. Remodelling is the only normal physiologic mechanism for altering bone structure in adult skeleton. Helps in maintaining bone tissue. However, leads to net loss of bone in elderly (*i.e.* osteoporosis).

2.6 FRACTURE FIXATION

Use of plates, screws, and wires was first documented in the 1880s and 1890s. Early surgical fixation initially was complicated by many obstacles, such as infection, poorly conceived implants and techniques, metal allergy, and a limited understanding of the biology and mechanics of fracture healing [46]. During the 1950s, Danis and Müller began to define the principles and techniques of internal fixation [47]. Over the past 40 years, advancements in biological and mechanical science have led to contemporary fixation theories and techniques [48,49].

Biomaterials have been defined *e.g.* as nonviable materials used in medical device and intended to interact with a biological system [50]. Many types of biomaterials are used, including metals, alloys, ceramics, polymers, composites and glasses. Various individual products are also available: heart valves, joint prostheses, dental implants, etc.

In the development of medical implants, many considerations of mechanical properties (strength, endurance), functionality (interaction between the implant and the body) and implant-specific design. Of course, the properties mentioned above are specific to each implant type and have to be considered case-by-case. For instance, both a hip implant and a heart valve have to be durable, but a hip implant has to be hadr to break and wear resistant, whereas a heart valve has to have good anti-thrombotic properties [51].

2.6.1 Metal implants

Stainless steel (SS) and titanium (Ti) are the principal metals used in trauma surgery. Cobalt-chromium (CoCr) alloys are used typically for joint replacements.

Stainless steel is commonly used because it is cheap, with adequate ductility, yield and ultimate strength. Titanium has advantages (less fatigable, greater modulus of elasticity, more biocompatible) but also disadvantages (expensive, sensitivity to stress raisers *e.g.* scratches, low tensile strength; not for lower limb). Some peo-

ple are hypersensitive to nickel or chromium, which limits the use of SS or CoCr alloys.

A short description of the metals used in trauma surgery:
Stainless steel (SS): A surgical alloy 316L SS contains chromium (13-15.5 %), nickel (17-19 %), and carbon (0.03 %). Nickel provides corrosion resistance and stabilizes the crystalline structure, chromium provides an oxidized surface reducing corrosion. The hardness of steel can be increased by the addition of carbon, up to about 0.65 percent.
Titanium: Titanium is used in 1-4 purity forms. Adding oxygen makes implants stronger and more brittle. Also alloys (*e.g.* Ti6Al4V including 6 % aluminium and 4 % vanadium) are used to increase strength and and corrosion resistance.
Cobalt-chromium (CoCr): CoCr is used in replacement implants due to its high wear-resistance and low corrosion rate, but seldom in trauma devices.

Risks of metal implants

Corrosion: Several types of corrosion will affect metals installed into human body; Galvanic corrosion (electrochemical currents when two dissimilar metals are in contact), crevice corrosion (variations of tension), stress corrosion (high-stress gradients) or fretting corrosion (micromotion abrading the surfaces).
Fatigue failure: Fatigue failure results of repetitive loading below the ultimate strength may cause eventually failure of the implant. Endurance limit is the stress at which the material will not fail even after several million cycles of loading. For example, endurance limit is 900 MPa and 520 MPa for cold-forged 316L SS and Ti6Al4V, respectively.
Creep: Creep is defined as progressive deformation of a the metal over time, under constant load.
Stress shielding: Stress shielding is caused by a harder and denser implant made of metal or hard plastic, which have the tendency

to absorb the stresses exposed to the body. Thus, the implant will disrupt bone's natural remodelling (Wolff's law). Thus, tissues surrounding the implant are shielded from stress impact and they will begin to disintegrate or to be reabsorbed.

2.6.2 Bioresorbable implants

Principal bioresorbable polymers in orthopaedics are polyglycolic acid (PGA) and polylactic acid (PLA). Bioresorbable impants are nor discussed further in this thesis. However, some notes of the use of these kind of implants include:

- Mechanical properties: low in strength, this can be improved by reinforcing.
- Non-reinforced resorbable implants: tensile strength 30-70 MPa. (Note: reinforced PLA 450 MPa.)
- Degradation by hydrolysis: when molecular weight is reduced to 5000 Da, foreign body reaction in body supersedes. Loss of strength in 1 month - 1 year. Resorption in 3 months - 6 years.
- Use is controversial: no removal needed, less stress shielding, no metal toxicity. However, as drawbacks of the material: expensive, low strength, foreign body reactions, synovitis.

Pena *et al.* [52] conducted a study to compare metallic and resorbable screws. They proved that the insertional forces and pull-out strength of the metallic screws were significantly higher than that of the bioresorbable screws.

To conclude, the feasibility of bioresorbable implants in orthopedics may be increased by improving the mechanical properties of the bioresorbable materials before they can be used for fracture fixation.

3 Biomechanics of screws

3.1 ANATOMY OF SCREWS

Bone screws are a basic component of modern internal fixation. They can be used independently or in combination with particular types of implants. The common design of a screw (see Fig. 3.1) consists of a tip, shaft, thread, and head. A round screw tip requires pretapping, whereas a fluted screw tip is self-tapping. The screw shaft is located between the head and the threaded portion of the screw. The screw thread is defined by its major or outer (thread diameter) and minor or root (inner or shaft diameter) diameters, pitch, lead, and number of threads. The distance between adjacent threads is the pitch, and the pitch diameter is defined as the mean diameter of major and minor diameters.

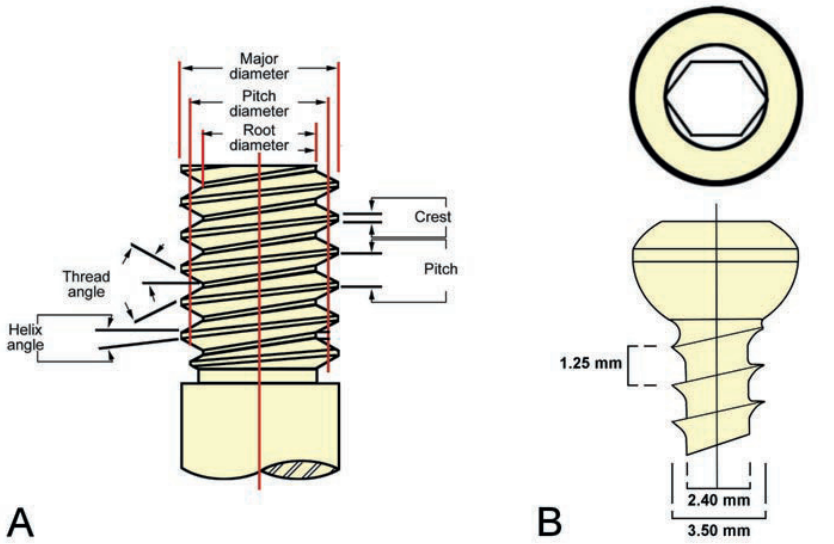

Figure 3.1: A) Screw anatomy with definitions. B) Dimensions of cortical bone screw used in the present study. (Modified from [53].)

The root diameter determines the screw's resistance to failure (tensile strength). Screws are referred to by their major thread diameters, bone type for intended use (cortical or cancellous, determined by pitch and major or minor diameters), and proportion of thread (partially or fully threaded).

Pitch, the distance between adjacent threads, affects purchase strength in bone. Greater pitch increases bone material between the threads but decreases the number of threads per unit of distance.

3.2 SCREWS IN FRACTURE FIXATION

Several forces are involved with screw insertion and tightening (see Fig. 3.2). Torque is applied through the screwdriver to the screw head in a clockwise rotation to advance the screw in the predrilled path; this advancement produces a circumferential force along the thread. Pretapping the screw hole theoretically reduces microfracture at the thread-bone interface but requires an extra step for insertion. Self-tapping screws have the advantage of eliminating a step during screw insertion, thereby decreasing operative time. The fluted design of the screw cuts a path in the predrilled hole, eliminating the need for tapping. Insertion torque and pull-out strength are reported comparable for tapped and self-tapping screws, however, also differences are found in *in vitro* models [13, 54, 55]. The fluted portion of the screw tip has less thread contact with the bone, so slight protrusion at the opposite cortex is recommended [56].

Two basic types of screws available for the variability of bone density are cortical and cancellous screws. Cortical screws are designed for compact diaphyseal bone, whereas cancellous screws are designed for the more trabecular metaphyseal bone. Cortical screws have a smaller major (thread) diameter, decreased pitch, and a shallower thread than cancellous screws.

For cortical screws, the drill diameter is slightly larger than the root (shaft) diameter of the screw. Axial tension is created with impingement of the screw head on the cortex or plate, generating tension through the screw. To optimize these forces, screws should

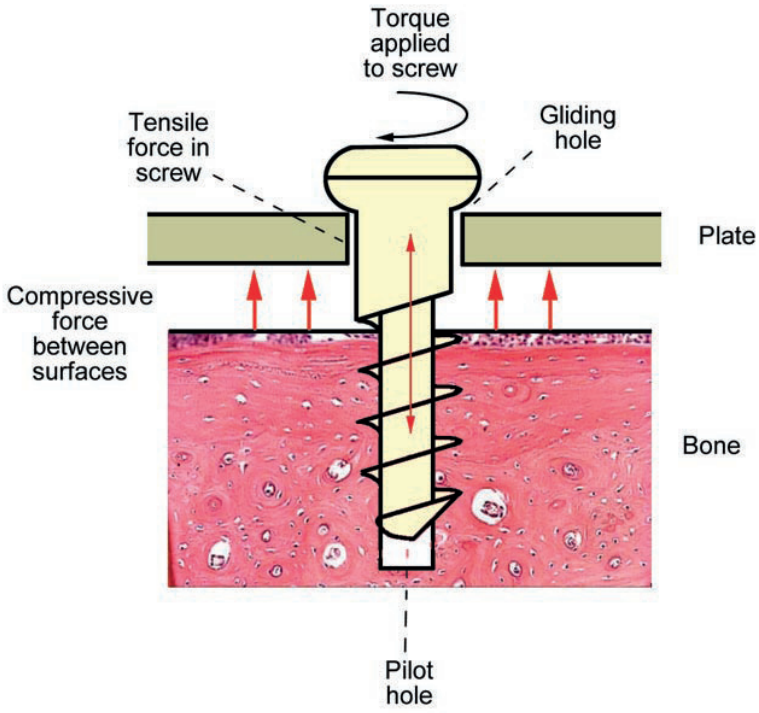

Figure 3.2: Mechanism of conventional plate fixation by generating compression between the plate and the bone for stability. (Modified from [53].)

ideally be inserted at 80 % of the torque needed to cause them to strip. An estimated 2500 – 3000 N of axial compression force can be applied to the small fixation screw of diameter 2.5 – 4.5 mm. Over time, the amount of compressive force decreases slowly as the living bone remodels to the stress; however, the fracture healing time is usually shorter than the time it takes for substantial loss of compression and fixation [27].

The aim of surgical intervention is to anatomically reduce and stabilize the fracture securely, while causing the least possible interference with healing [27].

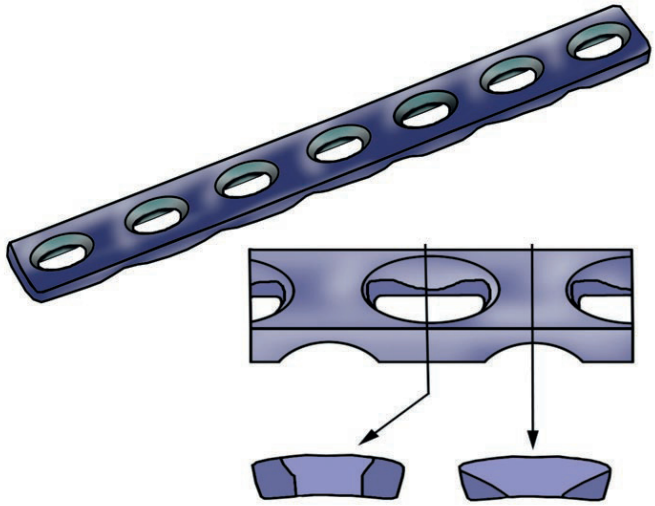

Figure 3.3: A design of a fixation plate used together with fixation screws in plate fixation. (Modified from [53].)

Conventional plate fixation (Fig. 3.3) requires use of several types of tools and implants:

Drills are used in many ways in trauma surgery, for example drilling preholes for screws. Optimum drill speed is low (750 – 1250 rpm). The most common reason for drill failure is bending.

Screws break because of two reasons: excess of torque during insertion or by bending. After implantation, bending of the screw occurs secondary to a loose plate or bone loss due to delayed or non-union. The bending and shear strength is mainly determined by core diameter of the screw.

Self-tapping screws have cutting flutes at the tip of the screw. The use of self-tapping screws reduces operation time, and impaction of bone around the thread during insertion increases hold. However, cutting flutes reduce area of thread; pull-out strength may be reduced by 10 % if threads are not advanced through the distal cortex. Also insertion torque is increased and there is a mild increase in temperature during insertion.

Plates are typically used to achieve compression. The strength of a plate is defined by $S = BH^3$ (B = width, H = height). Plate failure is usually due to fatigue and is more likely if there is a gap between bone and the plate. Plates are provided in various sizes and shapes for different bones and locations. The screw holes in a dynamic compression plate are shaped with an angle of inclination on one side away from the center of the plate. When tightened, the screw head slides down the inclination, causing movement of the bone fragment relative to the plate, resulting in compression at fracture sites.

In addition to conventional plate fixation system, a modern locking plate have been introduced for enhancing fixation stability. Firstly introduced in the 1990s, the concept takes advantage of unicortical, self-tapping screws with threaded screw heads that lock into the screw hole of the plate and minimize soft tissue disruption. These new plate designs offer advantages for certain fractures, such as proximal and distal humerus, distal radius or distal femoral fractures as well as osteoporotic bone. However, biomechanical and outcome studies are still recommended for these designs [53].

3.2.1 Implant removal

The complication rates following metalware removal vary from 3 to 40%. The principal problems are neurovascular damage and refracture. The forearm plates are most frequently associated with problems within removal. Refracture is caused by two principal phenomena [27]:

1. Removing a screw leaves a stress riser in the bone. If the size of the hole is significantly greater than 20 - 30 % of the diameter of the bone, the weakness rises exponentially. Thus, small screws (such as 3.5 mm) are recommended in the forearm, for example.

2. Bone under a plate demineralizes, either by stress shielding phenomenon affected by a stiff implant or bone necrosis caused

by the plate occluding the periosteal blood supply.

Examples of retrieved screws and plate are presented in Fig. 3.4 showing typical findings on implants after their removal from human body.

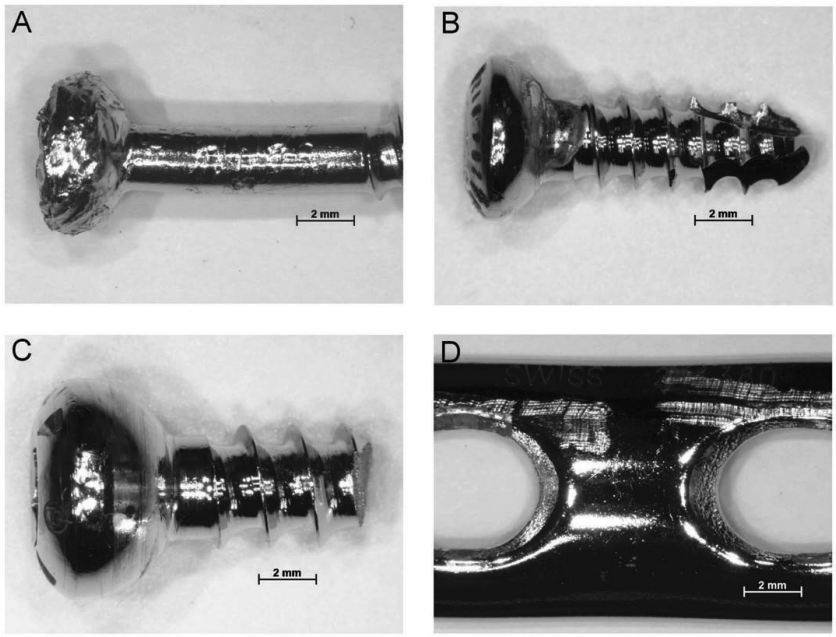

Figure 3.4: Stainless steel fracture fixation screws retrieved from patients indicating various defects on screws. A) Defects caused by removal tools. B) Tissue residue and deformation inducing different types of corrosion. C) Screw which was fractured during removal and D) Fixation plate showing *e.g.* marks of deformation.

3.3 BIOMECHANICAL TESTING OF SCREWS

Complex forces affect screws once inserted into bone. Hence, the screw itself has to be strong enough to accommodate the forces. Bending strength of a screw can be expressed in terms of section

modulus (Z):

$$Z = \frac{(\pi d^3)}{32} \tag{3.1}$$

Thus, in bending screw strength is proportional to the third power of the minor (inner) diameter (d) [57,58]. Various methods can be used to test the strength of the fracture fixation. In addition to the strength of the fixation, properties of the bone (or test material), bone-screw interface and the screw itself can be concluded from the biomechanical tests [1,2,14,27,46,59–61]. There are some limitations in each test type and thus, combinations of the tests discussed in the following sections should be used when evaluating the holding properties of the fixation.

3.3.1 Pull-out testing

Pull-out testing of screws in the axial direction is derived from their principal mode of operation in conventional plate fixation; the screws are axially preloaded to generate compression between bone and plate. Protocol for pull-out testing is simply to fix the sample block to a test machine and to withdraw the screw from the test material along the screw axis with a constant displacement speed. According to ASTM standards speed of pull-out should be 2.54 mm/min. However, pull-out rates of 0.1 - 5 mm/s have been reported depending on the screw and material type [11,62,63]. Maximum pull-out force (in newtons, N) required for screw removal is to be recorded. In this study, axial displacement speed of 5 mm/min was used in Paper IV.

Screw pull-out strength can be affected by several factors. Bone composition (density) is the primary determinant of screw fixation. The total surface area of thread contact to bone (root area) is another factor in pull-out resistance.

Main factors with respect to screw design are thread depth and the major diameter. However, also other variables such as length of cortical purchase, pitch height and thread angulation contribute to the pull-out behaviour. In any case, screw pull-out causes failure of the bone as well.

In a simplified model, the pull-out strength of a screw can be determined as a product of shear strength of the materials the screw is inserted into and the surface area of the deformed material [64]:

$$F_{pull-out} = S_{shear} \times A_{shear} \tag{3.2}$$

where:
$F_{pull-out}$ = predicted pull-out force (N)
S_{shear} = material ultimate shear stress (MPa)
A_{shear} = thread shear area (mm^2) = $\pi L D_{major}$
L = length of thread engagement in material (mm)
D_{major} = major thread diameter (mm)

In the case of a screw

$$F_{pull-out} = \left[S_{shear} \times L \times \pi \times D_{major}\right] \times TSF \tag{3.3}$$

where:
TSF = thread shape factor $= 0.5 + 0.57735d/p$ (defined by the D732-90 ASTM standard),
d = thread depth (mm),
p = thread pitch (mm).

Thus, according to the equations above screw pull-out strength can be improved by *e.g.* increasing insertion depth or depth of threads of the screw.

3.3.2 Torsional testing

As a result for torsional testing of bone screws, the insertion torque after initial four revolutions with constant rotation speed should be presented according to ASTM standard F543 ('Standard Specification and Test Methods for Metallic Medical Bone Screws'). Most common, however, is to present peak torque values for testing through the whole sample block. In the case of *in vivo* animal models, peak removal torque is reported [3, 65–68]. *In vitro* rotation speed 5 rpm was used in this thesis. It must be noticed that the *in vitro* rotation

speed does not correspond to higher speed used in clinical operation theater.

Torsional forces during screw insertion have been shown to correlate with pull-out strength, especially with synthetic bone blocks [69,70]. However, pull-out studies conducted in cadaver bone did not always show strong correlations between insertional torque and pull-out strength [12,71,72].

Insertion torque depends on screw type, diameter and design [4,5,13], hole preparation or pretapping [9,10], and of course, material properties (such as bone mineral density in the case of bones) [11,70,73].

Maximum insertional torque (M_m) can be defined by an equation proposed by Brånemark *et al.* in 1997 [74]:

$$M_m = \tau_m \times A_T \times (\%bc) \times r \tag{3.4}$$

where:

τ_m = interfacial shear stress in torsion at maximum torque (N/mm^2)
A_T = total fixture surface area (mm^2)
$\%bc$ = percentage of A_T in direct contact with bone
r = mean thread radius (mm).

Ivanoff *et al.* [65] suggested a simplified version to be used calculating shear strength of the bone:

$$M_m = \tau_m \times \pi \times d \times s \times r \tag{3.5}$$

where:

τ_m = interfacial shear stress in torsion at maximum torque (N/mm^2)
d = mean diameter of the implant (mm)
s = length of the implant in bone (mm)
r = mean thread radius (mm).

Typically, there are practical limitations in calculating exact values of both maximum insertion torque or shear strength, because; in the case of equation 3.4 one has to determine the surface area

in direct contact with bone, whereas in the case of equation 3.5 interfacial area is estimated by geometrical constants. Estimation of insertion torque, however, needs exact values of shear stress of the test material, which, especially in the case of human bone, is very difficult.

3.3.3 Fatigue testing

Methods for testing of fatigue properties were introduced already in the 1980's to study implant-bone cement interface [75] as well as a system for studying fatigue properties of porous surfaces [76]. However, there are only a few studies describing fatigue behaviour of cementless screws so far [77–82].

Besides of increasing number of cementless joint replacements, the common use of screws and other fixation devices are of great interest also with respect to their endurance properties. Their survival in long-term use affects significantly the fixation stability, infections, mechanical rigidity of the bone or need for additional operations. Thus, one should assume that more effort will be spend on fatigue testing.

3.3.4 *In vivo* testing

Several researchers have reported studies on screw fixation properties *in vivo*. In many cases, not only the biomechanics (*i.e.* fixation strength) of the screws in clinical–related cases [8,65,83–87] is tested but also effects of novel coatings are to be studied [17, 67, 88–92]. Especially, osteoconductive coatings (*e.g.* hydroxyapatite or titania) have been under close investigation during the years. The aim of these studies is most commonly to improve implant stability via better adhesion on the implant in the bony tissue.

Typical implant sizes in the case of fixation devices are small in diameter (for example 2.0 mm, 2.7 mm or 3.5 mm) as well as the animals used in the tests, *i.e.* rats or rabbits [65,74,93–96]. However, there are also studies simulating better human biomechanics with the use of sheep or even equine [6, 15, 55, 67, 89, 97–99].

Most of the studies in the past, simple pull-out tests have been conducted [9, 62, 64, 100, 101]. However, also the importance of removal torque is appreciated recently [70, 102]. Typically, histological or clinical findings are also addressed and correlated to fixation strength parameters. Major clinical parameters include especially bone mineral density (BMD), cortical thickness and cortical bone area. In histological studies bone-implant contact area, new bone formation or inflammatory factors are studied [85, 103–110].

3.3.5 Evaluation of screw-induced damage in bone

Natural microdamage caused by fatigue can stimulate bone remodelling by initiating resorption by osteoclasts and new bone formation by osteoblasts [111–117]. However, in the case of internal fixation extensive bone damage may result in the weakening of the fixation leading to implant loosening. Insertion of internal fracture fixation devices, such as screws, mechanically weakens the bone around the screw during insertion and removal. Typically, microcracking occurs due to prolonged loading or fatigue, especially in elderly patients. In addition, the strength and stiffness of the whole bone are also decreased as the extent of microdamage increases [2, 118, 119]. Local frailty due to stress in a bone may lead to extended healing times or even worse, total failure.

A wide range of methods have been used to detect microdamage and cracking of bone. Typically, normal transmitted light microscopy on histological thin slices is used for damage and crack detection or for osseointegration studies [17, 65, 89, 103, 107, 120]. However, reflected light microscopy [121], acoustic emission methods [122], Raman spectroscopy [123] and lately also scanning electron microscopy (SEM) and micro-computed tomography (μCT) are also been utilized to detect and analyze damage formation in bone samples after insertion of screws or dental implants, for example [73, 124–126].

A summary of recent studies on cortical bone screw fixation is presented in Table 3.1. The list was limited to relevant studies with respect to this thesis. Thus, studies on *e.g.* pedicle or cancellous screws have been excluded.

Table 3.1: Examples of recent studies on various kinds of bone screw testing.*

Test type	Screw size and type	Test sample	Ref.
Insertion torque and pull-out			
Insertion torque and pull-out	1.5 and 2.0 mm Ti	PVC, wood, porcine	[127]
Insertion torque, μCT	1.6 and 2.0 mm Ti6Al4V	porcine	[73]
Insertion Torque	2.7 - 4.5 mm SS	cadaver and construct	[108]
Pull-out strength	3.5 mm SS	e-glass filled epoxy	[62]
Fatigue			
Fixation stability	6.5 mm SS	foam blocks, human cadaver	[128]
Fixation fatigue	2.7 mm SS	aluminium tube	[80]
Syndesmosis stability	3.5 and 4.5 mm SS	human cadaver	[82]
Screw fatigue	3.0 mm SS	PE tube	[81]
In vivo			
Insertion torque, microscopy	3.5 mm Ti6Al4V	dog	[17]
Light microscopy	3.0 mm Ti	rabbit	[107]
Removal torque, microscopy	3.4 mm Ti	rabbit	[95]
Light microscopy	3.75 mm Ti6Al4V	rabbit	[103]
Microdamage and osseointegration			
Light microscopy, SEM	several	human, dogs	[120]
Removal torque, microscopy	4.5 mm SS	sheep	[129]
SRμCT	2.2 mm Ti (dental)	rat	[125]
μCT	1.8 mm Ti (dental)	dog	[124]

* Additional abbreviations in the table:

PVC = polyvinyl chloride, PE = polyethylene, Ti6Al4V = titanium alloy containing 6 % aluminium and 4 % vanadium, SRμCT = Synchrotron Radiation-based μCT

4 Diamond-like carbon (DLC) coatings

4.1 INTRODUCTION TO DIAMOND-LIKE CARBON (DLC)

Diamond-like carbon (DLC) coating was invented in the early 1970s by Aisenberg and Chabot using ion beam to deposit DLC thin films [130]. DLC's superior properties of natural diamond, chemical inertness and mechanical hardness, makes it appealing to many researchers to develop coating methods and to explore fields of applications for DLC.

DLC coatings have been applied to several wear-resistant applications, such as medical prostheses, cutting tools or even to automotive industry [18,21,131–133].

4.1.1 Structure of DLC

There are several subgroups of carbon–related structures and/or coatings with various properties (see Table 4.1). It has been found out that mechanical and chemical properties closest to natural diamond is achieved by an isotropic disordered DLC coating with no grain boundaries [134].

Carbon can form bonds in several ways (*i.e.* crystalline and disordered structures) because it has three different bonding configurations (see Fig. 4.1) [134]. In the nature elemental carbon is usually found in one of its two allotropic forms, *i.e.* graphite and diamond. In graphite, three valence electrons enter trigonally directed sp^2 orbitals and form covalent bonds. The fourth valence electrons form a 2D electron gas and the sp^2 bonded planes interact via weak Van der Waals forces. In diamond, the carbon atom's four valence electrons are each assigned to a tetrahedrally directed sp^3 orbital, which

makes a strong covalent bond with an adjacent atom. The strong and equivalent covalent sp^3 bonds in diamond explain its extreme physical properties. In amorphous DLC coating, the carbon atoms are arranged so that no long range crystalline order is present.

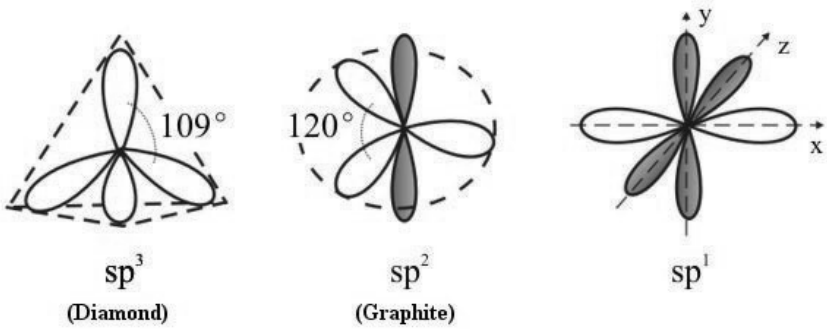

Figure 4.1: States of carbon bonding. (Modified from [134].)

Table 4.1: Some physical properties of various types of carbon–related materials [134].

	sp^3 (%)	*H* (%)	Density (g/cm^3)	Hardness (GPa)
Diamond	100	0	3.515	100
Graphite	0	0	2.267	0.2
ta-C	80-88	0	3.1	80
a-C:H (hard)	40	30-40	1.6-2.2	10-20
ta-C:H	70	30	2.4	50

The term DLC has been used as a general term for carbon coatings containing diamond-like bondings. The properties of the coatings differ from each other significantly depending on the sp^3 fraction, e.g. from soft polymer-like coatings to hard as diamond (see Fig. 4.2). Thus, the findings from the literature is hard to compare without exact information about the structure of the coating. In this

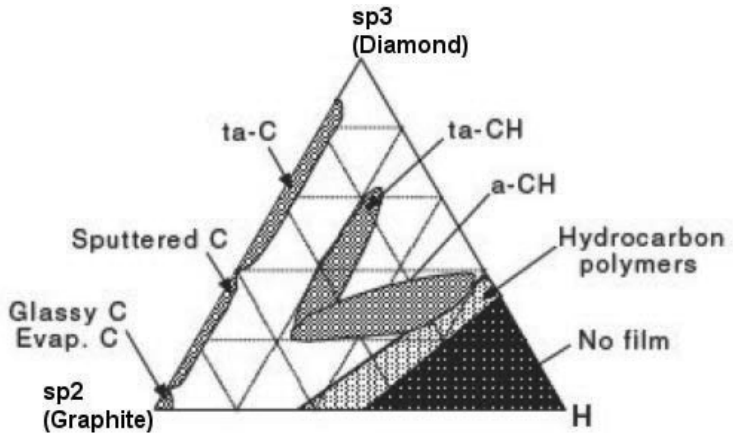

Figure 4.2: Phase diagram for various DLC films with respect to their sp^3 and sp^2 and hydrogen contents. (Modified from [134].)

study, high-quality DLC coatings with sp^3 fraction over 70% were produced and utilized [135].

The term tetrahedral amorphous carbon (ta-C) has been suggested for materials with high sp^3 fraction to distinguish it from the sp^2 bonded amorphous carbon (a-C). A term amorphous diamond (AD), is also been used instead of ta-C. AD refers to non-organized structure with a high percentage of diamond–like bondings. Furthermore, terms a-C:H and ta-C:H refer to materials containing significant amount of hydrogen [136–139].

In this study, term AD coating was used in Papers I-II, and in Papers III-IV term diamond-like carbon (DLC) was used. In this summary, the term DLC is used for simplicity. In the following chapters, application of DLC coating in fracture fixation screws and improvements in the insertional and removal torque as well as pull-out strength will be discussed.

4.1.2 Coating methods for producing DLC

There are also several kinds of coating methods to produce carbon coatings. Main categories are chemical vapour deposition (CVD)

and physical vapour deposition (PVD) methods. By chemical vapor deposition (CVD) methods relatively rough and brittle coatings containing small crystalline diamonds are formed, and thus, CVD methods are not suitable for producing wear-resistant DLCs.

A PVD method, filtered pulsed arc discharge (FPAD), was developed in the University of Helsinki, Diamond Group led by prof. Asko Anttila in the 1980s [135]. DLC coatings with superior properties could be prepared by this method that utilizes high-energy carbon plasma beams yielding high deposition rates and high-quality coatings (*i.e.* coatings with high amount of sp^3 diamond bonds). At the same time, even thick coatings up to hundreds of micrometers could be produced. In typical applications, the coating thickness less than a micron is adequate to modify surface characteristics of the product. However, FPAD is not easily applied to industrial scale, but is well suitable for basic research.

The FPAD deposition method has been built up in University of Eastern Finland by prof. Lappalainen and is was utilized for preparing DLC coatings in this study. A schematic representation of the FPAD unit is shown in Fig. 4.3. Procedure and details of coating process and parameters are described, *e.g.* in references [135, 140] but they are not discussed here.

Some further considerations related to FPAD method include the choice of substrate material; the substrate should be hard enough to withstand loads under thin (< 10 μm) coatings as well as it should chemically form carbides. The use of intermediate tantalum layer is developed so that a wider variety of substrate materials can be used as a substrate. Tantalum itself is biocompatible with low corrosion rate. A commonly used substrate for FPAD as well as for biomedical applications is stainless steel AISI316L.

DLC coatings can be also produced by laser ablation (LA) method, which utilizes intense laser beam directed towards a target to generate a plasma plume. Plasma is then transported to a substrate to produce thin films. Development of a novel LA method ”Ultra short pulsed laser deposition, USPLD” in the University of East-

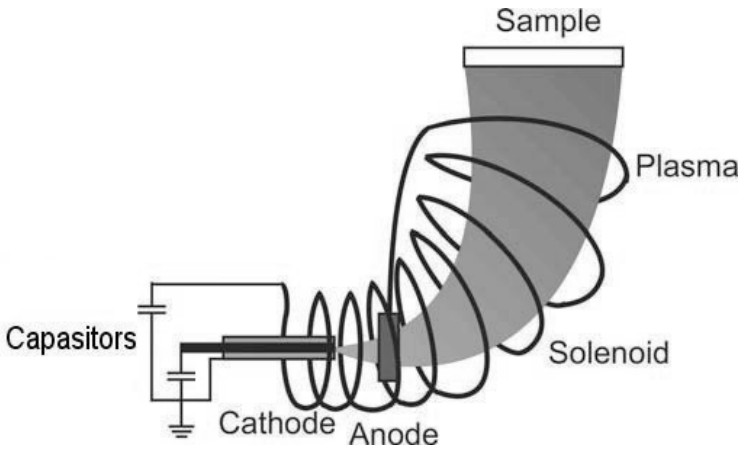

Figure 4.3: Schematic illustration of the FPAD coating system.

ern Finland has been succeeded in co-operation with the research group of prof. Lappalainen and an industrial partner (Picodeon Ltd, Helsinki, Finland).

Distinct feature of USPLD method is that there is no large compositional deviation from the target. Further, deposition of macroparticles is prevented by uniform conversion of the uttermost layer of the target to expanding plasma plume by short term pulses. Also, as compared to more conventional deposition methods, USPLD allows coating deposition of materials with high melting point. In addition, it does not produce film contamination and the stoichiometry of the target is directly transferred to the coating, and thus, also multicomponent targets can be used. [51].

Fundamentally, properties of high-quality DLC coatings (or AD) produced by FPAD are further improved by novel USPLD coating method. Thus, compositional (*i.e.* diamond-like) and surface properties (*e.g.* smoothness) of the coating are gained with USPLD.

4.2 DLC IN BIOMEDICAL APPLICATIONS

DLC coatings have been tested for biomedical applications in numerous studies. One of the first fields of research was the sliding surface of joint replacements, *i.e.* hip prostheses tested by joint simulator testing [18, 139, 141, 142]. DLC proved to offer an alternative for metal-on-metal prostheses with metal ion release problems as well as metal-on-polyethylene prostheses with high wear rate problems. Among other superior findings, the use of DLC coatings proved even 1 million times reduction of wear rate. [18]. However, yet DLC coatings have not reached to the market in this field. This may be due to poor outcome of some coatings used in sliding surfaces, *i.e.* in hip or knee prostheses, where delamination of the coating was observed in the long-term clinical use (*e.g.* Oxinium; Smith&Nephew Co).

DLC surfaces have excellent haemocompatibility and DLC–coated cardiovascular implants such as heart valves, blood pumps and stents are available on the market. In addition, DLC has been tested successfully as a coating for guidewires, urinary tract catheters, orthodontic archwires etc. [143]

In this study, we have tested the performance of DLC coating on fracture fixation screws with *in vitro* mechanical tests. Considerations of insertional torque, pull-out strength and frictional properties have been addressed. After this initial set of tests, the aim is to continue for *in vivo* testing.

In summary, DLC is proven to have outstanding tribological properties and it is tolerated well by the body. It has been demonstrated that DLC does not trigger any adverse effects on attached cells and thus, DLC can be considered to be biocompatible by *in vivo* and in many *in vitro* experiments [143].

4.2.1 Characterization of DLC

In addition to clinically relevant studies on durability and wear described above, basic characterization of chemical, mechanical and tribological properties of DLC is essential during the development

process of novel coatings. In this summary, details of variety of characterization methods are not discussed. A list of various characterization methods utilized in the literature is shown in Table 4.2 [144–146].

Table 4.2: Summary of methods utilized to characterize DLC coatings.

Characterization method	Information achieved
Contact angle measurement	Surface wettability (hydrophobicity vs. hydrophilicity); cell and/or dirt adhesion ability
Profilometer	Surface roughness
Optical microscope	Surface finishing, cracking; visual outlook
Raman spectroscopy	Chemical composition; fraction of sp^2 and sp^3 bondings
X-ray photoelectron spectroscopy (XPS)	Elemental composition
Scanning electron microscopy (SEM)	Detailed surface finishing; voids, pits, microcracking (Elemental composition when equipped with *e.g.* energy dispersive spectrometer, EDS)
Transmission electron microscopy (TEM)	Atomic level structure; crystallization, amorphous structure; (fraction of sp^2 and sp^3 bondings when equipped with electron energy loss spectrometer, EELS)
X-ray diffraction spectroscopy (XRD)	Crystallinity
Atomic force microscope (AFM)	Surface morphology
Nanoindentation	Surface hardness and elasticity
Pin-on-disc tribometer	Coefficient of friction (CoF), wear rate
Pin pull-out testing	Adhesion of the coating
Scratch tester	Adhesion of the coating, cracking sensitivity
Impedance tester	Electrical properties

4.2.2 Biocompatibility of DLC

Biocompatibility of the DLC has been studied *in vitro* by *e.g.* cytotoxicity studies, cell adhesion studies, mutagenicity evaluation and various *in vivo* studies [107,146].
As mentioned earlier, DLC has been proven to have excellent haemocompatibility [19] allowing it to be used even in cardiovascular applications. However, in the present study biocompatibility is not investigated, and thus, not discussed further.

4.3 CONCLUSION

Diamond-like carbon (DLC) coatings have several advantageous properties that can be utilized in various applications requiring high resistance to corrosion or wear, for example. Especially novel USPLD coating method can produce high-quality, thick and smooth DLC coatings that are promising materials of the future also in industrial scale. Further development related to *e.g.* surface texturing or modifications of the coating will even improve and make it possible to tailor the properties of the coating as needed in specific application.

5 Aim of the study

The present study aimed at improving the knowledge about potential of diamond-like carbon (DLC) coatings in biomedical applications, especially in bone fracture fixation screws, as well as about the methods suitable for *in vitro* biomechanical testing and analysis. Furthermore, relationship between different biomechanical parameters and their effect on screw fixation strength was investigated.

Specific aims and methods of the thesis can be stated as:

- Paper I: Develop and validate a testing equipment for screw insertion and removal *in vitro*. Furthermore, to study the effect of DLC coating on insertion torque using synthetic and natural materials.
- Paper II: Investigate the effect of DLC coating on insertion torque in human cadaver bone, and to study the correlation between bone mineral density (BMD) and insertion torque.
- Paper III: Utilize various analyzing methods (including optical microscopy and μCT) to detect screw–induced damage in human bone and to study the effect of DLC coating on bone damage.
- Paper IV: Increase knowledge about factors affecting fixation strength (especially effect of friction) and validate substitute materials modeling human bone for biomechanical testing.

6 Materials and methods

6.1 BONE SCREWS

6.1.1 Self-tapping cortical bone screws

In Papers I, II and IV self-tapping cortical bone screws were studied. Screw material was stainless steel (AISI 316L; Zimmer Inc., Warsaw, USA), and similar screws are commercially available for clinical use, too. Self-tapping screws are a common type of orthopaedic screws used in uni- or bicortical fracture fixation. Drilling of a hole into a bone (or test block) is needed prior to screw installation but the hole does not need pretapping due to cutting flutes in the screw tip that make a sharp cut into the material. Self-tapping screws are nowadays recommended by the manufacturers to be used in the operation theater. There have been discussion in the literature, whether the self-tapping screws weakens fixation strength of the screws but clear indication of this not available [1, 4, 13].

Screws of two sizes with outer (major) diameter of 2.7 mm (inner diameter 2.0 mm) and 3.5 mm (2.5 mm) were used in all above mentioned studies. Length of the screws altered from 30 mm in pull-out tests (Paper IV) to 60 mm in insertional tests with human bone (Paper II). The variation of the screw length has no relevance in these tests. Pilot holes into the test blocks were drilled using sizes recommended by the manufacturers, *i.e.* 2.0 mm for 2.7 mm screws, and 2.7 mm for 3.5 mm screws.

6.1.2 DLC coatings of the screws

In Papers I and II, filtered pulsed arc discharge (FPAD) method was utilized for coating half of the screw sets (see Fig. 6.1). The method is widely studied and the coatings produced with the specific equipment at University of Eastern Finland (previously Uni-

versity of Kuopio) have been reported to yield in high-quality DLC coatings with excellent hardness and wear resistance, for example [18,20,142].

However, novel USPLD method was utilized in Paper IV. Coating method which is well–controlled and suitable also for tailored coatings was developed and applied. Nevertheless, the USPLD equipment is reported to produce high-quality coatings of DLC and other materials, as well [147,148].

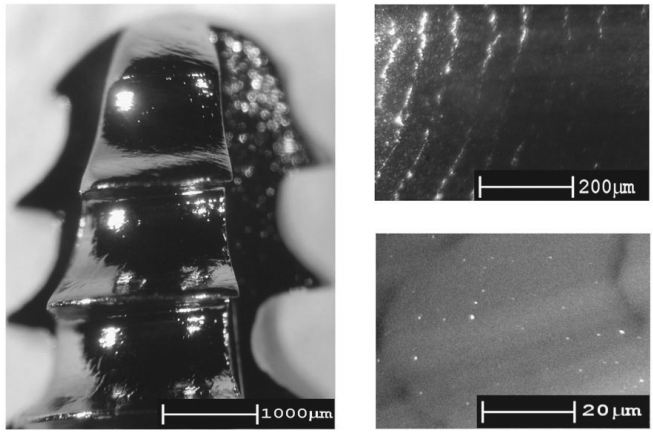

Figure 6.1: A tip of a DLC–coated self-tapping bone screw is shown on the left (screw diameter 3.5 mm). The inserts show optical micrograph (upper) and SEM (lower) of the screw with different magnifications.

6.2 BONE AND BONE SUBSTITUTES

Various material blocks were utilized in the Thesis for studying screw fixation properties. Practical issues concerning availability, mechanical homogeneity or preservation justify the use of standard materials in addition to human bone specimen. Human bone would otherwise be the best choice for simulating clinical use of the screws.

6.2.1 Human cadaver bone

The cadaveric bone specimens used in Papers II and III were donated by Jyväskylä Central Hospital (Jyväskylä, Finland). Bone specimens were harvested from the distal end of the femoral shaft. The specimens were 6-8 cm in length, 4-6 cm in diameter and included the whole bone, *i.e.* cortical and trabecular components (see Fig. 6.2). The samples were stored in buffered saline and kept frozen at all times if they were not under study. The number of human bone specimens was eight from which seven were from males and one was from a female. The samples were divided into two groups with a mean age of 34 years (range 25-41 years, $N = 4$) and 75 years (range 73-77 years, $N = 4$; including the female sample), respectively.

The use of human bone samples in the present study is conceded by permission of the Finnish National Authority for Medicolegal Affairs (TEO, 1781/32/200/01).

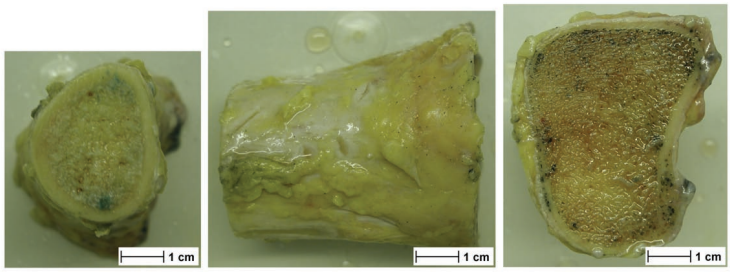

Figure 6.2: A cadaver femur used in the experiments imaged from different points-of-view.

6.2.2 Other materials used as bone substitutes

Blocks of various materials were used to model human bone in present studies. Justification of bone substitutes include, *e.g.* biomechanical, ethical and practical considerations. In contrast to cadaveric bones, synthetic test specimens have low variance in mechanical properties and are readily available with well specified proper-

ties. Most critical concerns are related to preservation of the specimens and variation in the mechanical properties of the cadaver bones. Furthermore, there is no risk of contamination or decomposition with the synthetic materials. Thus, in literature synthetic materials or other natural materials have been used in biomechanical research [64, 69, 108, 127, 149–152]. In the present study, the following bone substitutes were used

- Paper I: polytetrafluoroethylene (PTFE), wood blocks (Scotch pine), and porcine and bovine bone

- Paper IV: polymethyl-metacrylate (PMMA), polyacetal (POM) and E-glass filled epoxy (Sawbones; Pacific Research Laboratories, Inc., Vashon, USA)

All the above materials have been used previously *e.g.* in similar studies [64, 69, 108, 127, 149–152]. Specifically, PMMA and POM was chosen because of respective difference in tensile strength and density, so that their effect on screw fixation could be analyzed (see Table 6.1).

Table 6.1: Comparison of mechanical properties of test blocks used in the studies. PMMA = polymethyl-metacrylate, POM = polyacetal, PTFE = polytetrafluoroethylene and Sawbones = trade name for E-glass filled epoxy (Pacific Research Laboratories, Inc., Vashon, USA). Data adopted from [2, 153, 154].

	Tensile strength σ (MPa)	Elastic modulus E (GPa)	Density ρ (mg/cm^3)
Human bone	133	10 - 15	1.2
PMMA	65	3.0	1.4
POM	74	3.0 - 3.3	1.1
Sawbones	90	12.4	1.7
PTFE	21 - 35	0.4 - 0.8	2.2
Scotch pine	102	12	0.5

6.3 EQUIPMENT FOR BIOMECHANICAL TESTING

6.3.1 Insertion torque testing

In Paper I, a custom-made apparatus for insertional testing was designed, constructed and validated. The apparatus consisted of two parallel steel shafts mounted on a solid steel plate allowing linear movement of the support stand with a drive motor (Alcatel Dunkelmotoren, Bonndorf, Germany) and a torque transducer (Torqsense E300/RWT; Sensor Technology, Banbury, UK). An analogue voltage signal proportional to the torque value was transferred to a computer and displayed; the data were analysed using the WinDMM 300 program (Appa Technology Corporation, Taiwan). Special care was taken to assure perfect alignment of the screw along the axis of the stand (see Fig. 6.3). Noticeable improvements to previous reports [8, 11, 12, 155] were achieved by continuous and adjustable motor control and signal recording. The apparatus fulfilled the standard ASTM F543 ('Standard Specification and Test Methods for Metallic Medical Bone Screws') requirements, and the system was used also in Paper II.

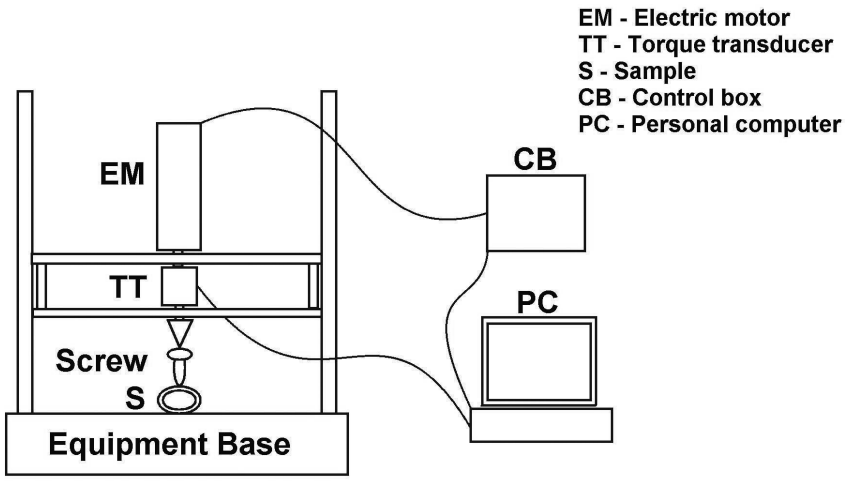

Figure 6.3: Schematic illustration of the developed test equipment for torque measurements.

In Paper IV, an enhanced set-up for testing of insertion torque was introduced. In this construction, a commercial test device (Instron 8874; Instron Co, Norwood, MA, USA) was modified for torsional tests of bone screws: a drive motor was attached to the piston of the equipment allowing precise axial load control during the testing. Torsional forces (*i.e.* torque) was also measured continuously with corresponding load cell and software from Instron. Also this equipment fulfills the same standard requirements as above, but with even improved reproducibility.
In the latter tests, screw insertion was carried out in diluted bovine serum with a total protein content of 24 mg/ml and standard additives to prevent microbial activity. The additives included Penicillin-streptomycin solution (EuroClone S.p.A., Siziano, Italy) and EDTA-disodium salt (Merck KGaA, Darmstadt, Germany). Natural environment and lubrication in the human body was simulated with the use of diluted serum.

The main test parameters required (used during the tests) by the standard ASTM F543 include:

- Continuous recording of torque (data sampling at least with 2 Hz with our equipment)
- Resolution of recorded data 10 % of measured value (our equipment capable of 0.01 Nm)
- Rotation speed 1-5 rpm (constant speed 5 rpm used in present studies)
- Axial load less than 1.14 kgf [load of 1.14 kg] (adjustable and controllable in our equipment)

6.3.2 Pull-out testing

In Paper IV, pull-out tests for the screws were performed in the standard bone substitute materials in addition to insertion torque. The same mechanical testing device (Instron 8874; Instron Co, Norwood, MA, USA) was modified for screw pull-out tests with the

help of special clamps for specimen attachment. Standard protocols with a constant speed on 5 mm/min was performed in displacement control. The data measured with a 1 kN load cell (accuracy 1 % of reading) was continuously recorded.

6.3.3 Tribological testing

In Paper IV, friction between test blocks and stainless steel or DLC–coated stainless steel was tested by using a pin-on-disk apparatus described in standard ASTM G99-95. For a pin AISI 316 stainless steel balls 6 mm in diameter (density: 7.96 g/cm3, Brinell hardness: 160-190) were used mimicking the screw material (Goodfellow Cambridge Ltd., Huntingdon, UK).
In the tests, the sample was placed on a rotated holder while the ball was attached to a lever with a dead weight (load). Digital force signal from a strain gauge was recorded and a coefficient of friction (*CoF*) was determined. The diameter of the sliding track was 4.5 mm and sliding speed 3.5 mm/s with applied load 9.8 - 79.0 g were used. Relative slow sliding speed was used to simulate *in vitro* testing condition for torque measurements as per standard ASTM F543. For the same reason, friction during the initial 50 revolutions (sliding distance 71 cm) was determined for each axial load. Tests were carried out in diluted bovine serum with standard additives as described above. Especially in tribological studies, it has been reported that the testing conditions (especially lubrication) have significant effect on friction [18,19,132]. Thus, the use of serum is well justified.

6.4 OTHER CHARACTERIZATION METHODS

6.4.1 Histological processing and analysis

Shortly described, after screw insertion and removal (in Paper II) cylindrical bone samples were prepared from each of the screw insertion sites for Paper III. Cylindrical samples were acquired using a hollow drill bit with a diameter of 10 mm. Subsequently, the cylin-

drical samples were post-fixed in 10 per cent phosphate-buffered formalin, dehydrated in increasing concentrations of ethanol, and embedded into histological resin (polymethyl-methacrylate, PMMA). For histological examination, slices perpendicular to the screw installation axis were then cut with an Exakt 310 CP microsaw (Exakt Vertriebs GmbH, Norderstedt, Germany), and ground polished with an Exakt 400 CS grinding system (Exakt Vertriebs GmbH, Norderstedt, Germany). The thickness of the final thin sections for optical microscopy was between 22 and 30 μm. Finally, the sections were stained with 1 % toluidine blue and examined under optical microscope with normal transmitted light.

Simple quantitative analyses were performed on the optical microscopy data acquired by a photomicroscope (Nicon FXA; Nikon Co, Tokyo, Japan) using AnalySIS software for Windows (version 3.2, Soft Imaging System GmbH, Münster, Germany). The periphery and diameter of the screw hole, and area of the damage were determined from the optical microscopy images and used as histomorphometric data.

6.4.2 Peripheral quantitative computed tomography, pQCT

In Paper II, a high-resolution pQCT scanner XCT2000 (Stratec Medizintechnik GmbH, Pforzheim, Germany) was used to determine the geometrical and density parameters for each of the bone samples. The pQCT scanning was performed with unfrozen specimens. The whole specimen was scanned with a slice thickness of 2 mm and a pixel size of 0.2×0.2 mm^2.
The cross-sectional images of the bones were analyzed using Geanie software (version 2.1; BonAlyse Oy, Jyväskylä, Finland) that automatically identifies different components of bone tissue and assesses densities and geometrical parameters. Tissue types in the pQCT scans were separated in the analysis by preset density thresholds; voxels with density values above 710 mg/cm^3 were considered as cortical bone, values between 180-710 mg/cm^3 as trabecular bone and values below 180 mg/cm^3 as soft tissue. The same

threshold values were used by Russo *et al.* [156]. (Images of analyzed slices at different levels of a bone sample presenting only the cortical bone are shown in Fig. 6.4.)
The relevant parameters which were taken into account in this study were cortical bone mineral density (BMD) and cortical bone area (CBA). Cortical BMD is a good general indicator of bone material properties and the CBA is a good measure of total cortical bone mass and a valid marker of bone resistance against compressive and tensile loads [156, 157]. CBA was determined as the cross-sectional area of the voxels with a density higher than 710 mg/cm^3.

Furthermore, in Paper III, the geometrical data of the bone specimens, *i.e.* cortical thickness (ThC), polar moment of inertia (I_{pol}) and cross-sectional cortical bone area ($CSAC$) were determined and the correlations between insertional properties and geometrical parameters were analysed.

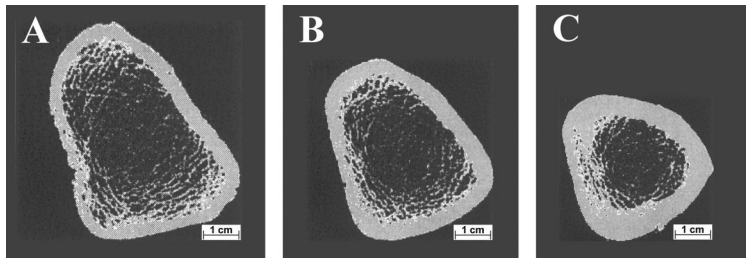

Figure 6.4: pQCT slices from different levels of a cadaver bone sample showing only the cortical bone tissue as grey colour. Transverse images of a cadaveric bone are: (A) from the distal end of the femoral shaft, (B) from 3 cm proximally from location (A), and (C) from the femoral diaphysis.

6.4.3 Scanning electron microscopy, SEM

In Papers II and III, scanning electron microscope (ESEM-TMP XL30; Fei Company, Eindhoven, The Netherlands) was utilized to study the quality of the DLC coating and microfractures of the bone samples. The equipment is capable of imaging in low-vacuum mode nonconductive samples such as embedded bone blocks without ad-

ditional treatments. Fairly low magnifications (50x - 2000x) were used during these studies.

6.4.4 Micro-computed tomography, μCT

In addition to SEM imaging, the remaining bone blocks (after histological sample preparation in Paper III) were scanned with a high-resolution Skyscan 1172 μCT unit (Skyscan, Kontich, Belgium) using a 6 mm pixel resolution. Also the corresponding screws were imaged with the μCT to obtain detailed information about these screws. Image reconstruction, processing, and analyses for μCT images were performed with the software package provided by Skyscan.
The μCT image analysis was carried out by predefining a region of interest (ROI) surrounding the screw hole in the bone blocks and by determining the damage volume (empty space) over a defined height. The corresponding volume of the screw was also determined and subtracted from the total damage volume. The damage volume was defined using the formula

$$V_D = (n_{total} - n_{bone} - n_{screw}) \times V_V \times h \tag{6.1}$$

where:

V_D = damage volume (mm^3)
n_{total} = total number of voxels within ROI
n_{bone} = number of voxels defined as bone within the ROI
n_{screw} = number of voxels in the screw in the corresponding ROI
V_V = volume of an individual voxel
h = height of the analysed ROI (h = 0.6 mm)

This method has not yet been widely used in similar studies, excluding few reports on dental implantology [124,158,159]. However, the interest on using μCT for non-destructive evaluation of bone-implant interface and structures for acquiring three-dimensional (3D) data is increasing. Especially, the method would provide also quantitative tools for structural and interfacial analysis.

6.5 STATISTICAL ANALYSES

Throughout the thesis, SPSS software (SPSS, Inc., Chicago, IL, USA) was used in statistical analyses. Significance level of $p < 0.05$ was considered as significant.

In Paper I, the mean torque and standard deviation were calculated for each sample block, rate of rotation and screw sizes, respectively.

Difference in torque and geometrical data (*i.e. BMD* and *CBA*) between young and old patients' bones were studied in Paper II by performing a Student's t-test for independent samples. For determining the correlations with respect to the same parameters, 2-tailed Pearson's correlation coefficient was calculated. The significance of different surface modifications were compared by One-way ANOVA.

In Paper III, Pearson's two-tailed correlation was calculated for the histomorphometric, insertional, and geometric data. The significance of difference between DLC–coated and non–coated screws were calculated using Student's t-tests. A post hoc statistical power analysis (two-tailed) was performed for the histomorphometric, insertional, and geometric parameters, with respect to screw surface modification as well as for the age of the patient.

One-way ANOVA was used to evaluate differences in insertion torque and pullout strength for different materials in Paper IV. Student's t-test was used for comparison of the effect of surface modification (DLC vs. SS). Pearson correlation analysis (2-tailed) was performed to evaluate correlations between different parameters (*i.e.* materials' mechanical properties and screw fixation strength).

7 Results

7.1 DEVELOPMENT OF TESTING EQUIPMENT AND PRELIMINARY STUDIES ON EFFECT OF DLC COATING

Results in Paper I show high reproducibility acquired by the custom-made equipment. Improvements achieved by the equipment as compared to previous studies include continuous rotation and torque recording. Table 7.1 shows the effect of rotation speed on torque, as well as low variation in the results.

Table 7.1: Insertion torque (τ) values with various rotation speeds in homogenous material (polytetrafluoroethylene, PTFE) and natural material (Scotch pine) for 2.7 mm and 3.5 mm screws, respectively. $N = 6$.

Rotation speed r (1/min)	PTFE: $\tau_{2.7mm}$ (Nm)	PTFE: $\tau_{3.5mm}$ (Nm)	Wood: $\tau_{2.7mm}$ (Nm)	Wood: $\tau_{3.5mm}$ (Nm)
2.5	0.08 ± 0.02	0.13 ± 0.02*	0.14 ± 0.02	0.17 ± 0.03*
5	0.11 ± 0.02	0.18 ± 0.02	0.17 ± 0.03	0.26 ± 0.05
7.5	0.15 ± 0.03	0.17 ± 0.04	0.17 ± 0.02	0.28 ± 0.04
10	0.17 ± 0.05*	0.20 ± 0.03	0.18 ± 0.03	0.30 ± 0.05

Significant difference ($p < 0.05$, One-way ANOVA) that were found between rotation speed 5 rpm (required by ASTM F543) and higher or lower speeds for corresponding material and screw size are marked with an asterisk (*) in Table 7.1.

For DLC–coated screws, the torque values were on average 10–15 % lower compared with uncoated, otherwise identical, screws (see Fig. 7.1).

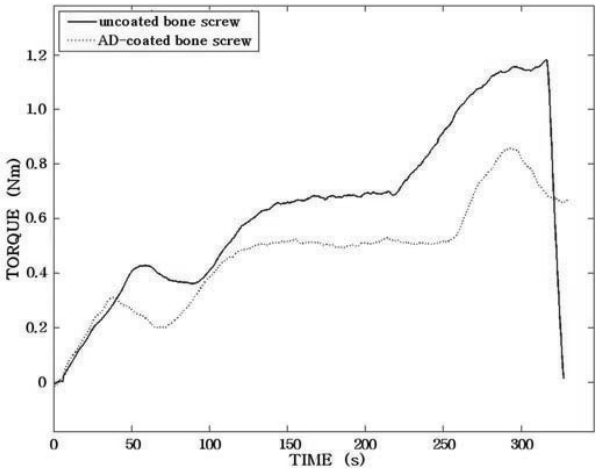

Figure 7.1: Insertion torque for two bone screws of diameter 2.7 mm, one with and one without coating. This test was applied to bovine femoral bone, which is significantly harder than human bone.

7.2 EFFECT OF BMD AND DLC ON INSERTION TORQUE IN HUMAN CADAVER BONE

Adjusted insertion torque (adjusted for the diameter 3.5 mm by the mean of 3.5 mm/2.7 mm torque ratios) was significantly lower in the old persons' group than in the young persons' group (see Table 7.2). This finding is in good agreement with the similar significant differences in bone mineral density (BMD) and cortical bone are (CBA), respectively.

The linear correlation coefficient between BMD and adjusted maximum insertion torque was $R = 0.504$ ($p < 0.01$, Pearson 2-tailed). The cortical BMD is a good general indicator of bone material properties and it was determined exactly at the screw installation site [156,157].

In the case of cortical bone area (CBA), the correlation coefficient between CBA and adjusted maximum insertion torque was $R = 0.767$ ($p < 0.01$, Pearson 2-tailed). The resistance of bone against compressive and tensile loads can be estimated from CBA

value [156, 157], which also is indicated in high correlations of this study.

Table 7.2: Human bone properties in Paper II for young and old persons' groups, and insertion torque (τ_{in}) for both groups. (BMD = bone mineral density, CBA = cortical bone area, both determined by pQCT (peripheral quantitative computed-tomography)). p-values tested with t-test for independent samples.

	Old bone	Young bone	p-value
BMD	1130 ± 20	1190 ± 40	0.00
CBA	2.50 ± 0.50	3.00 ± 0.60	0.00
τ_{in}	0.35 ± 0.08	0.43 ± 0.10	0.02

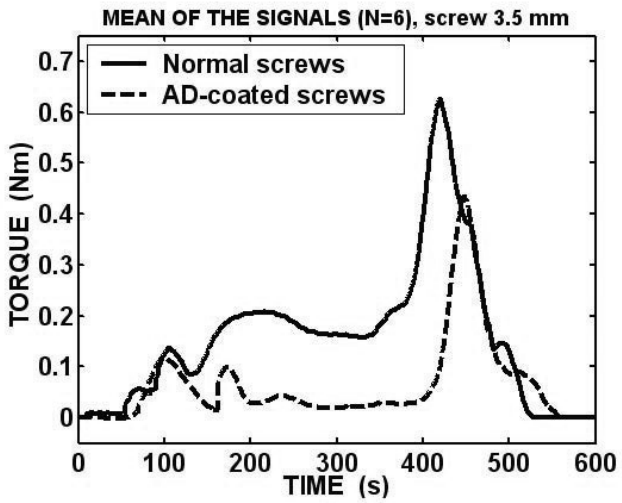

Figure 7.2: Mean insertion torque (N = 6) of DLC–coated (AD–coated) and non-coated screws of diameter 3.5 mm in human bone.

Major decrease in insertion torque was achieved especially with AD-coated screws which were polished after coating. At maximum, even 50 % lower torque values were obtained for DLC–coated screws than for as–delivered screws in the first cortex (see Fig. 7.2). Testing with amorphous diamond coated bone screws confirmed good durability of the coating, and no drastic delamination of the

coating was observed.

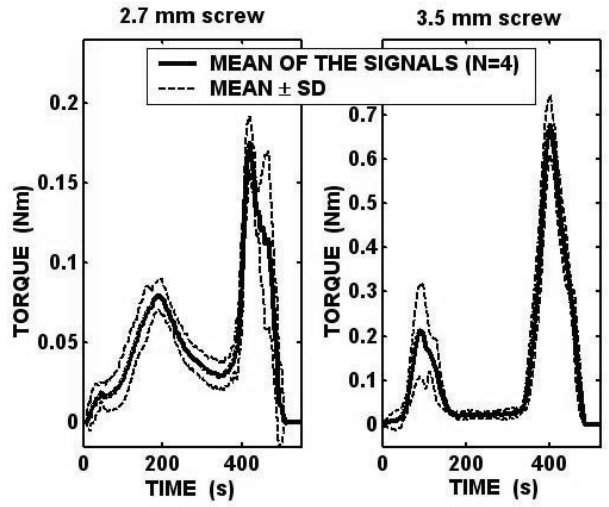

Figure 7.3: Mean insertion torque (± SD, N = 4) for screws of diameter 2.7mm (left) and screws of diameter 3.5 mm (right). Note the different scales in the y-axis.

The findings also suggest that the thicker screws cause plastic deformation in the first cortex resulting in very low torque between the cortices. Whereas in the case of thinner screws the elastic component in bone deformation is considerable and therefore, insertion torque between the cortices is relatively high (see Fig. 7.3).

7.3 SCREW-INDUCED DAMAGE IN HUMAN BONE AND THE EFFECT OF DLC COATING

The screw–induced damage obtained from optical microscopy images was defined as periphery and diameter of the screw hole and the area of damage, and they are referred as 'histomorphometrical parameters'. To determine the effect of surface modification and increase statistical significance, the images of the smaller screws (diameter 2.7 mm) were scaled to correspond to the size of the larger screws (diameter 3.5 mm).

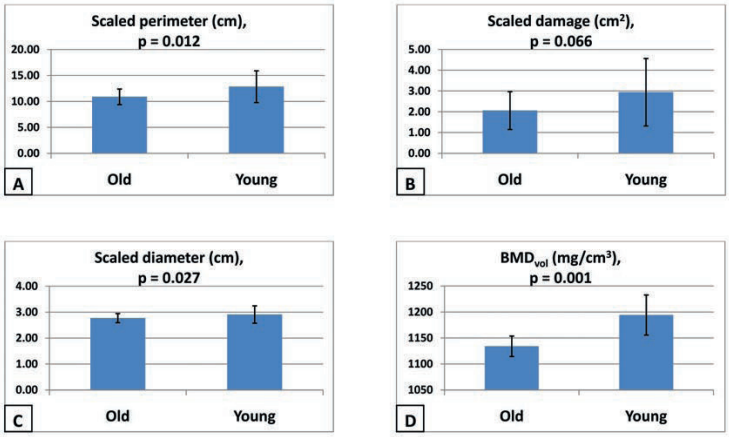

Figure 7.4: Bar plots ($\pm$ SD) of histomorphometric parameters and volumetric BMD presented with respect to the age of the patients: (a) scaled perimeter; (b) scaled damage; (c) scaled diameter; and (d) volumetric BMD. Significance (p-values, t-test) between the groups are presented, respectively.

The histomorphometric parameters were significantly higher for the bones of young patients (see Fig. 7.4). In particular, perimeter of the damaged hole was affected by bone mineral density (BMD_{vol}), which is consistent with the finding that BMD_{vol} showed a significant difference between the two age groups.

For the DLC–coated screws, the histomorphometric data had a positive correlation with the geometric data, *i.e.* cross-sectional cortical bone area ($CSAC$), polar moment of inertia (I_{pol}) and cortical thickness (ThC) (see Table 7.3). In particular, the polar moment of inertia (I_{pol}) had a significant correlation with all the histomorphometric parameters. However, there were no significant correlations between the histomorphometrical data and insertion torque (τ_{max} or τ_{cortex}). Furthermore, no significant differences could be seen in

the histomorphometric parameters between DLC–coated and normal screws.

Table 7.3: Pearson two-tailed correlation coefficients (and exact 2-tailed significance values p) between histomorphometric (scaled perimeter, scaled damage, and scaled diameter), insertional (maximum torque τ_{max} and torque in first cortex τ_{cortex}), and geometric ($CSAC$, I_{pol}, ThC) parameters. The coefficients are presented for DLC screws and normal screws, respectively. The data shown here represents both age groups; N=38.

	Scaled perimeter (AD, normal)	Scaled damage (AD, normal)	Scaled diameter (AD, normal)
$CSAC$	0.387 (p=0.113)	0.450 (p=0.061)	**0.559 (p=0.025)**
	-0.059 (p=0.871)	-0.199 (p=0.582)	**-0.817 (p=0.025)**
I_{pol}	**0.591 (p=0.010)**	**0.671 (p=0.002)**	**0.582 (p=0.018)**
	0.362 (p=0.304)	-0.264 (p=0.461)	-0.417 (p=0.352)
ThC	0.358 (p=0.145)	0.331 (p=0.179)	0.430 (p=0.096)
	-0.359 (p=0.310)	-0.099 (p=0.785)	-0.484 (p=0.271)
τ_{max}	0.262 (p=0.295)	0.232 (p=0.353)	0.098 (p=0.719)
	-0.028 (p=0.939)	0.167 (p=0.645)	-0.314 (p=0.492)
τ_{cortex}	0.004 (p=0.987)	0.058 (p=0.819)	0.182 (p=0.501)
	-0.267 (p=0.456)	0.117 (p=0.747)	-0.326 (p=0.475)

Some bone tissue debris became stuck in the cutting flutes of the self-tapping screws during the insertion and part of this debris stayed in the hole even after screw removal (see Fig. 7.5 (C)). The bone debris affected the automated deformation analysis obtained from the μCT images. The deformation volume analyses from μCT images showed large variations in their results. The volume of the tissue deformation was determined and this provided complementary data for image analysis of the optical microscopy images. The average damage volume (defined by equation 6.1) for the whole analysed sample set was 2.7 $\pm$ 1.6 mm^3 (N = 6). As a reference; screw volume with a similar analysed height is 3.4 mm^3.

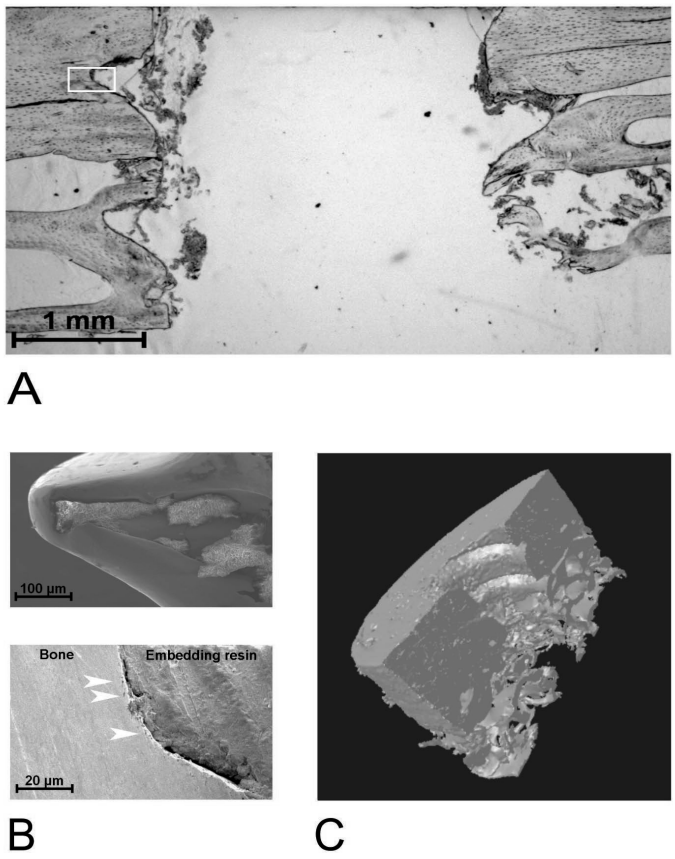

Figure 7.5: Figure of microscopic (A. optical microscopy, B. scanning electron microscopy) and C. μCT findings of bone damage.

7.4 FACTORS AFFECTING SCREW FIXATION STRENGTH AND SUBSTITUTE MATERIALS MODELING HUMAN BONE

Screw insertion torque and pull-out strength were highly affected by mechanical properties of bone substitute test blocks. Interestingly, pull-out strength was highly correlated to elastic modulus of the test blocks, whereas insertion torque was highly correlated

to tensile strength of the test blocks (see mechanical properties of the test blocks in Table 6.1). However, mechanical properties and fixation strength parameters of cadaver bone did not correlate as well as in the case of synthetic materials. Specifically, the highest insertion torque values were recorded for E-glass filled epoxy (Sawbones) and lowest for human cadaver bone. Insertion torque was significantly higher ($p < 0.05$, One-way ANOVA) for polymethylmetacrylate (PMMA) and Sawbones than for cadaver bone. In the case of pull-out strength, Sawbones had highest values and PMMA lowest values (see Fig. 7.6).

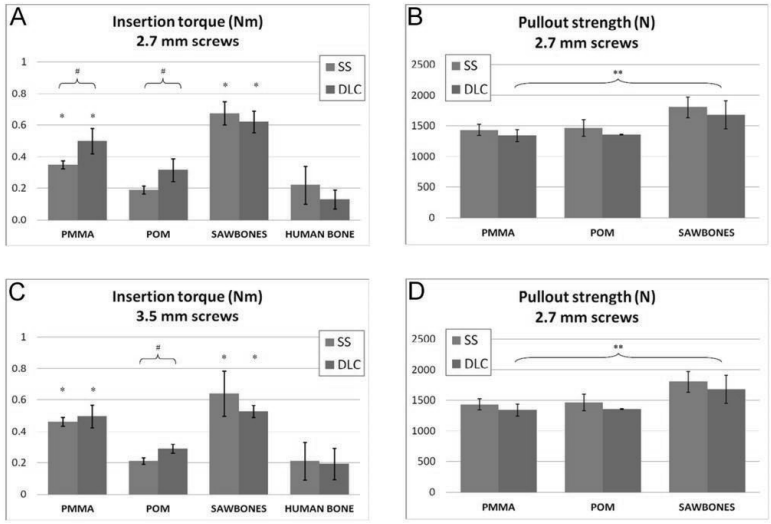

Figure 7.6: A and C) Insertion torque in test blocks for non-coated and DLC–coated SS screws with diameter 2.7 mm and 3.5 mm, respectively. B and D) Pull-out strength in bone substitute test blocks for non-coated and DLC–coated SS screws with diameter 2.7 mm and 3.5 mm, respectively. ** indicates significant difference from human bone. One-way ANOVA, $p < 0.05$; # indicates significant difference between SS and DLC. t-test, $p < 0.05$; ** indicates significant difference between PMMA and Sawbones. One-way ANOVA, $p < 0.05$. No significant differences were found between SS and DLC.*

Coefficient of friction (*CoF*) was determined for human cadaver bone and three bone substitute materials against stainless steel (SS)

and diamond like carbon (DLC) coated stainless steel. In both cases, CoF was significantly ($p < 0.05$, ANOVA) lower in bone than in the substitute materials (see Table 7.4). However, no significant difference in these short term tests of CoF was achieved by DLC coatings.

Table 7.4: Coefficient of friction (μ) for stainless steel (SS) and diamond-like carbon (DLC) against bone or bone substitutes (PMMA, POM and Sawbones). * indicates significant difference from all other materials; One-way ANOVA, $p < 0.05$.

	μ_{SS}	μ_{DLC}
Human bone	0.09 ± 0.04*	0.09 ± 0.04*
PMMA	0.31 ± 0.01	0.38 ± 0.06
POM	0.19 ± 0.01	0.20 ± 0.03
Sawbones	0.29 ± 0.03	0.31 ± 0.03

CoF correlated strongly to screw insertion torque. For SS screws, correlation coefficients were R = 0.652 and 0.763 for 2.7 mm and 3.5 mm screws, respectively (Pearson 2-tailed). Similarly for DLC–coated screws, correlation values of R = 0.597 and 0.812 were determined for 2.7 mm and 3.5 mm screws, respectively. However, pull-out strength of bone substitute materials did not strongly correlate to CoF. For SS screws, correlation coefficients R = 0.304 and 0.061 and for DLC–coated screws R =-0.112 and -0.307 were determined (for 2.7 mm and 3.5 mm screws, respectively; Pearson 2-tailed).

8 Discussion

8.1 POTENTIAL OF DIAMOND-LIKE CARBON (DLC) COATINGS FOR FRACTURE FIXATION SCREWS

Insertion torque of the screws is mainly determined by the screw design, friction at the interface and the density of the bone. Thus, the use of a smooth DLC (AD) coating which has a low coefficient of friction against most of the materials [18,131,160] may lead to low torques, reduced heat elevation during screw installation and furthermore, less thermal damage to tissues [14]. The relationship between temperature elevation and torque has also been studied [161], and the results suggest that there is a strong (R^2 = 0.55) correlation between insertion torque and heat generation.

Additionally, insertion torque determines the force with which bone fragments are held together [2]. Therefore, it is important to control the insertion torque in order to prevent bone from stripping or the screw from failing. Consequently, the use of DLC coating in bone screws should diminish bone deformation, produce a rigid fixation and enable faster healing.

Generally, low coefficient of friction (*CoF*) was aimed for in this study with the developed DLC coatings yielding to lower torque. However, the coating can also be modified to have moderate or even high *CoF* to accommodate needs in specific applications [162, 163]. In the case of fracture fixation screws, excellent biocompatibility and low *CoF* is desired with stainless steel screws which are typically removed after bone's natural healing process, whereas titanium screws are left into the body in some cases and good osteointeraction and stability can be achieved by rough or patterned coating.

Already in preliminary testing with DLC–coated bone screws in Paper I the coating was found to have good durability and resulted in on average 10 - 15 % lower torque values compared with

uncoated screws in porcine and bovine bone samples.

In Paper II, the preliminary results were confirmed with human cadaver bone, and even with more convincing way; insertion torque in first cortex was reduced up to 50 % by DLC–coated screws. The findings with human cadaver bone also suggest that when using the thinner screws the elastic component in bone deformation is considerable and therefore, insertion torque between the cortices is relatively high. For the thicker screws, the bone deformation is more in the plastic area, *i.e.* the yield point of the stressstrain curve is exceeded, structure of the bone tissue is plastically deformed, and insertion torque between the cortices is very low. Thus, the maximum torque is determined by the failure strength of bone and not so much by the friction at the sliding surfaces (see Fig. 7.3).

However, even minor reduction in insertion torque allows use of smaller screws which, in turn, results in decreased amount of damage, faster healing and regain of bone strength. The use of large screws and drilling holes will also weaken the bone strength even by 10 – 40 % [2,14,164].

The common recommendation is that an ideal coating must be stable, bioactive and osteoconductive but also dense and adherent. In addition to reduced insertion torque also reduced total energy required in screw insertion were hypothesized in this study. The beneficial effect of a smooth and bioinert DLC coating would then be related to decreased friction and energy used for bone deformation during the screw insertion. Significant differences in the amount of bone damage were not found between DLC–coated and normal screws in Paper III. This may be due to large variation in the results. However, the borderline of the holes drilled by the screws were qualitatively different for coated and non-coated screws; for the borderlines were typically rough or smooth for DLC–coated and non-coated screws, respectively. This could be partly explained by sliding due to lower friction for DLC–coated screws and by cutting for non-coated screws, and thus, it can be related to elastic and plastic deformation of bone during installation and removal.

For some fracture fixation devices and situations, the long-term consequences of bone-screw fixation are relatively unimportant, *e.g.* since the cortical screws are intended to be a temporary support during the critical healing period of fracture [17], or in case of infection [165], fatigue failure of the implant [166], or several pain [167]. The use of DLC coating would result in high fixation strength in a short healing time due to less damage. This would be an advantage for fracture fixation, particularly in cases of osteoporotic bone or an unstable fracture.

DLC coating has potential to adjust the coefficient of friction (*CoF*) as shown in earlier studies [18, 19]. Especially, novel USPLD method can produce smooth coatings with tailored surface properties, which may yield to beneficial applications also within biomedical science.

In Paper IV, *CoF* of SS against human bone and standard materials was not affected by a smooth DLC coating in bovine serum lubricated setup. The tribological properties (both dynamic and static) of DLC films have been thoroughly investigated in the past showing that their *CoF* highly depends on experimental conditions [18,19,94]. We consider that the use of bovine serum in testing of *CoF* simulates well the clinical environment.

Further, DLC coating had a controversial effect on screw fixation properties in Paper IV. Interestingly, insertion torque was lower for DLC–coated screws with Sawbones and human bone. These materials have the highest tensile strength and elastic modulus (see Table 6.1 in Chapter 6). Thus, DLC coating seems to perform better with stronger materials and can be concluded that in such materials elastic deformation in dominant. Insertion torque seems even to increase with DLC–coated screws in standard materials with lower strength. This phenomenon may be due to carbon - carbon interaction between polymers (*i.e.* PMMA and POM) and DLC. In composite materials (*i.e.* Sawbones or human bone) this interaction will not occur.

Despite of the promising results and findings in our *in vitro*

studies presented here, also *in vivo* testing is needed to study the long-term behaviour of screw materials and the stability of attachment to bone with different surface treatments. Many studies have reported that corroded surfaces can easily make late removal of bone screws difficult and can lead to screw failure as shown in retrieval studies [3–6, 89]. Thus, it is important to study long-term effects of the DLC coatings so show potential also in clinical use, as it has been proven to have good resistance against corrosion [131].

8.2 BIOMECHANICAL TESTING AND ANALYSIS METHODS FOR ORTHOPAEDIC RESEARCH

8.2.1 Biomechanical testing of screw fixation strength

Although the measurement of screw torque is a straightforward task, care should be taken to avoid systematic errors such as those due to poor alignment. Correct alignments is necessary to prevent severe side loading on the screw, which may even lead to failure of the screw. In the set-ups presented in this thesis, alignment was achieved with a freely moving holding device, which resulted in high producibility.

According to the ASTM standard F543, the insertion torque is defined as the maximum reading during the initial four revolutions of the screw and the removal torque is defined as the maximum reading during four revolutions when reversing the direction of rotation. However, this is a difficult task, especially without continuous recording and constant rate of rotation. Thus, the the presented set-ups allow observation of oscillations in torque, *e.g.* due to torsional stiffness of the screw and stick-slide motion in the case of thin, long bone screws especially at low rates of rotation and high torque. Furthermore, the devices developed in during the thesis have been mimicked by other researchers [108].

Insertion torque is reported to be mostly affected by screw design and geometry, such as core diameter and thread pitch [108]. In this thesis, different types of screws were not studied, but it was

found out that the insertion torque increased roughly as the square of the screw diameter; this agrees with the simple rule based on the size of the screw.

Pull-out tests, however, is derived from the screws' principal mode of operation in conventional plate fixation; the screws are axially preloaded to generate compression between bone and plate. This compression should result in sufficient friction to transfer loads that act orthogonal to the screw axis. The results from the pull-out tests are regarded primarily as a measure of bone (material) quality around the fixture. This is due to screw thread design transferring stresses to the surrounding material [94]. Thus, the reduction in modulus of elasticity, tensile modulus or tensile strength of the material would clearly impact the fixation strength, stiffness and durability of orthopaedic implants also in clinical use [152]. As demonstrated in literature, tightening the screw to high torque levels past the yield point of bone can cause damage leading to compromised holding strength [168].

Screw pull-out strength is affected by several factors related to material block or screw design. Mechanical properties of the test block as well as the total surface area of screw thread contact to bone are fundamental factors in pull-out resistance. Major screw–related factors are thread depth and the major diameter. However, also other variables such as length of cortical purchase, pitch height and thread angulation contribute to the pull-out behaviour.

This thesis showed that the pull-out strength in bone substitute materials was highly correlated with elastic modulus, tensile strength and density of test block. Screws with larger major diameter (3.5 mm) had significantly higher pull-out strength than the smaller screws (2.7 mm). In pull-out, there were no significant differences with respect to surface modification. As in the case on insertion torque, no other screw design factors were studied.

8.2.2 Other analysis methods for orthopaedic research

Various imaging methods were utilized in the thesis to collect information on bone, screw–induced damage or quality of the DLC coating.
Peripheral quantitative computed tomography (pQCT) was used in this study to determine volumetric BMD of the cadaver bones with high resolution. pQCT was found to be feasible, easy to use and even analysis of the measurement was done automatically and objectively with a corresponding software. The resolution and information achieved by the method is well suitable for both research and clinical purposes. The ability to determine BMD at an actual screw installation site was an advantage in this study and the correlation between BMD and screw insertion torque was clearly shown. For other kinds of studies, the ability to separate different tissue types and to determine their areas would be useful, too.

For histological and histomorphometrical studies, it was noticed that normal light microscopy is a sufficient tool for damage evaluation with a sufficient pixel resolution. Although the methodology for preparing the thin slices for optical microscopy is well-known and documented [65, 103, 120], there is always the risk of introducing artefacts during the cutting and grinding of thin sections, which is clearly shown in scanning electron microscopy (SEM) images, too. Despite this, by far the most popular method of microcrack detection has been transmitted light microscopy [111].

Methods for histomorphometrical analysis of stained sections are often ”in house standards” and they are time and money consuming [103]. Thus, an automated tool for micro-computed tomography (μCT) image analysis was also studied in the thesis. The main advantage of using automated tools is less time consumption and thus, a possibility to use larger sets of samples to gain statistically significant results [17, 65, 103]. In this study, μCT provided a powerful visualization tool for non-destructive structural imaging of whole sample in 3D. However, thresholding in the image analysis, bone residue in the screw hole and pores in bone tissue create

uncertainties in the analysis and the results of the μCT data.

Large variation in the bone deformation results of the present study can be partially explained by the findings of several previous studies in bone-implant contact surface, which is found to be 40 - 50 % in the cortical passage [65, 104, 169]. Additionally, a stick–friction phenomenon noticed and shown in our data, and also suggested by Kincaid [108] would support our findings: bone is damaged from a larger area after sticking and thus, no difference in damage could be detected between surface modifications.

One interesting approach would be utilizing correlative light - electron microscopy for studying *e.g.* bone damage. In this method exactly same location could be analyzed with low and high magnification which increases accuracy and reproducibility of the findings. Nevertheless, sample preparation and processing would, again, give limitations for the acquired information.

8.2.3 Effect of mechanical properties of specimen blocks on screw fixation strength

Cadaveric bone specimens would be the most biomechanically appropriate model for simulating clinical case. However, the bones have a number of associated difficulties, such as decomposition and variability in mechanical properties. The literature demonstrates variability in geometric and material properties within and between different cadaver subjects, which is not optimal for biomechanical testing. Thus, the use of bone substitute materials have been justified and recommended for *in vitro* tests by many researchers [62, 69, 152]. The findings of this study also illustrate the difficulty in choosing a material resembling human bone for biomechanical testing. Each substitute material has pros and cons with respect to the type of mechanical testing.

In Paper IV it was shown that the screw pull-out strength in bone substitute materials was highly correlated with elastic modulus, tensile strength and density of test block. The pull-out strength

for POM was statistically similar to PMMA and Sawbones with both screw sizes. The results from the pull-out tests are regarded primarily as a measure of bone (material) quality around the fixture. This is due to screw thread design transferring stresses to the surrounding material [134]. Thus, the reduction in modulus of elasticity, tensile modulus or tensile strength would clearly impact the fixation strength, stiffness and durability of orthopaedic implants also in clinical use [152]. Pull-out strength was not studied for human bone in this thesis.

Screw insertion torque, in contrast, was highly correlated to elastic modulus, tensile strength and coefficient of friction of the test blocks. The insertion torque for POM was statistically similar to human cadaver bone with both screw sizes. Yet, insertion torque is reported to be mostly affected by screw design and geometry, such as core diameter and thread pitch [108]. In general, our results were in agreement with previous studies with similar materials and screws [62,108,152].

One would suspect from the materials' mechanical parameters (see Table 6.1) that strong and stiff bone yields in high insertion torque. However, the mechanical testing reveals contradictory findings; insertion torque did not show good correlation to material mechanical properties when results of human bone were included. This is most likely due to inhomogeneous structure of bone, as well as due to biological elements (lipids, proteins) in bone which affect beneficially the sliding properties of the screws.

Within a set of human bone specimens, it was demonstrated (Paper II) that the insertion torque correlated to bone mineral density (BMD). There was a clear indication that in the case of bone, the denser the material is the higher insertion torque yields. However, differences in density of bone and substitute materials do not directly correspond to differences in insertion torque, respectively.

Interestingly, significantly lower CoF values were recorded for human bone than for substitute materials against either SS or DLC. This finding needs better attention in further studies to understand sliding at the bone-implant interface and the role of bone compo-

nents. A comprehensive mechanism study is still needed to fully understand the relationship between surface roughness and sliding properties of materials. Thus, a proper model for human bone was not found with respect to interfacial sliding properties.

As the bones' geometrical properties are discussed in detail, strong correlations were found in Paper III between insertional torque and both cortical thickness (*ThC*) and cross-sectional cortical bone area (*CSAC*). This finding suggests that the same critical parameters that determine bone strength and its resistance to fracture [119, 170–173] determine also screw insertion torque. Thus, geometrical parameters from clinical imaging (*e.g.* X-rays) could be utilized for estimation of screw size for fracture repair.

Positive and strong correlation was found between the bone histomorphometric (damage) parameters and polar moment of inertia (I_{pol}) in Paper III. However, the correlations between damage parameters and *ThC* or *CSAC* were not significant. This may be due to large variation in results but also due to the fact that damage caused by the screws is also affected by several other factors, such as geometry and design of the screws.

To summarize, according to the present studies standard materials can be utilized as bone substitutes for biomechanical studies in orthopaedics research. However, the appropriate material must be chosen by clinically relevant outcome of the test and composite nature of the material but not only by mechanical properties, such as density. Thus, clinically relevant tests using cadaver or animal bone specimens are still needed to gather comprehensive data for understanding mechanical factors at the bone–implant interface.

9 Summary and conclusion

The present study aimed at improving the knowledge about potential of diamond-like carbon (DLC) coatings in biomedical applications (*i.e.* bone fracture fixation screws) as well as the protocols for their biomechanical testing *in vitro*. Furthermore, relationship between different biomechanical parameters and their effect on screw fixation strength was investigated.

The following conclusions can be drawn:

- Insertion and removal torque can be measured with good reproducibility with the equipment developed in the thesis according to ASTM standard F543.
- DLC coating resulted in at maximum 50 % lower torque values compared with uncoated screws in the cortex of human cadaver bone. In homogenous standard materials decrease of insertion torque with 10 – 15 % was found. Furthermore, no significant difference was found in pull-out strength of the screws with and without the DLC coating in homogenous standard materials and thus, initial fixation stability of coated and non-coated screws is similar. Cyclic fatigue *in vitro* tests would be a next step to study long-term stability of the screw fixations.
- Microscopic analysis of histological sections provides a useful tool for qualitative and even quantitative analysis of screw - induced damage in bone tissue. μCT provides a method for nondestructive structure analysis and 3D imaging of the specimen, and thus, provides complementary information.
- *In vitro* testing is needed for initial testing of hypotheses, but one should also consider proper test material and type of biomechanical test for each application. In the case of bone

screws, testing of fixation strength is fundamental and can provide both screw–related and material–related information. This information may then help implant design and material choices for clinical applications.

- The improvement achieved by DLC coatings is expected to remain even in long-term use due to inertness and biocompatibility of the coating. However, *in vivo* animal models is required to confirm this hypothesis and to study osseointegration, implant stability, screw holding strength and removal torque. These tests may reveal the full potential of high-quality DLC coatings (or; amorphous diamond) for this particular type of biomedical use.

In general, necessity for surface modification by coatings is inevitable; interactions between biological environment and biomaterials occur on the materials surface, and the biological response to these extrinsic materials (foreign bodies) depends on the surface properties of the material. Specific challenges include, *e.g.* improvement of wear and corrosion resistance, influencing cell adhesion and growth, or modifying biocompatibility with blood.

Further development related to implant surfaces will include texturing or patterning surfaces, and preparing of modified coatings with tailored surface properties. As our general knowledge on interaction between cells and materials improves, current trend leans towards nanometer scale where tailoring even on molecular level will be possible.

Bibliography

[1] J. L. Cunningham, "The biomechanics of fracture fixation," *Curr Orthop* **15,** 457–464 (2001).

[2] M. Nordin and V. H. Frankel, *Basic biomechanics of the musculoskeletal system*, 3 rd ed. (Lippincott Williams & Wilkins, Philadelphia, 2001).

[3] P. R. Klokkevold, P. Johnson, S. Dadgostari, A. Caputo, J. E. Davies, and R. D. Nishimura, "Early endosseous integration enhanced by dual acid etching of titanium: a torque removal study in the rabbit," *Clin Oral Implants Res* **12,** 350–7 (2001).

[4] A. Kuhn, T. McIff, J. Cordey, F. Baumgart, and B. Rahn, "Bone deformation by thread-cutting and thread-forming cortex screws," *Injury* **26 (Suppl. 1),** 12–20 (1995).

[5] A. W. Kwok, J. A. Finkelstein, T. Woodside, T. C. Hearn, and R. W. Hu, "Insertional torque and pull-out strengths of conical and cylindrical pedicle screws in cadaveric bone," *Spine* **21,** 2429–34 (1996).

[6] M. Rocca, M. Fini, G. Giavaresi, N. N. Aldini, and R. Giardino, "Osteointegration of hydroxyapatite-coated and uncoated titanium screws in long-term ovariectomized sheep," *Biomaterials* **23,** 1017–23 (2002).

[7] K. Yokoyama, T. Ichikawa, H. Murakami, Y. Miyamoto, and K. Asaoka, "Fracture mechanisms of retrieved titanium screw thread in dental implant," *Biomaterials* **23,** 2459–65 (2002).

[8] W. W. Lu, Q. Zhu, A. D. Holmes, K. D. Luk, S. Zhong, and J. C. Leong, "Loosening of sacral screw fixation under in vitro fatigue loading," *J Orthop Res* **18,** 808–14 (2000).

[9] T. K. Daftari, W. C. Horton, and W. C. Hutton, "Correlations between screw hole preparation, torque of insertion, and pullout strength for spinal screws," *J Spinal Disord* **7,** 139–45 (1994).

[10] B. T. Oktenoglu, L. A. Ferrara, N. Andalkar, A. F. Ozer, A. C. Sarioglu, and E. C. Benzel, "Effects of hole preparation on screw pullout resistance and insertional torque: a biomechanical study," *J Neurosurg* **94,** 91–6 (2001).

[11] T. C. Ryken, J. D. Clausen, V. C. Traynelis, and V. K. Goel, "Biomechanical analysis of bone mineral density, insertion technique, screw torque, and holding strength of anterior cervical plate screws," *J Neurosurg* **83,** 325–9 (1995).

[12] M. Ueda, M. Matsuki, M. Jacobsson, and A. Tjellstrom, "Relationship between insertion torque and removal torque analyzed in fresh temporal bone," *Int J Oral Maxillofac Implants* **6,** 442–7 (1991).

[13] S. Yerby, C. C. Scott, N. J. Evans, K. L. Messing, and D. R. Carter, "Effect of cutting flute design on cortical bone screw insertion torque and pullout strength," *J Orthop Trauma* **15,** 216–21 (2001).

[14] A. Tencer and K. Johnson, *Biomechanics in orthopedic trauma. Bone fracture and fixation.* (Martin Dunitz Ltd, London, 1994).

[15] A. Moroni, P. Aspenberg, S. Toksvig-Larsen, G. Falzarano, and S. Giannini, "Enhanced fixation with hydroxyapatite coated pins," *Clin Orthop Relat Res* **346,** 171–7 (1998).

[16] K. Hayashi, N. Matsuguchi, K. Uenoyama, T. Kanemaru, and Y. Sugioka, "Evaluation of metal implants coated with several types of ceramics as biomaterials," *J Biomed Mater Res* **23,** 1247–59 (1989).

[17] J. H. Lee, H. S. Ryu, D. S. Lee, K. S. Hong, B. S. Chang, and C. K. Lee, "Biomechanical and histomorphometric study on the bone-screw interface of bioactive ceramic-coated titanium screws," *Biomaterials* **26,** 3249–57 (2005).

[18] R. Lappalainen, M. Selenius, A. Anttila, Y. T. Konttinen, and S. S. Santavirta, "Reduction of wear in total hip replacement prostheses by amorphous diamond coatings," *J Biomed Mater Res* **66B,** 410–3 (2003).

[19] R. Hauert, "An overview on the tribological behavior of diamond-like carbon in technical and medical applications," *Tribology International* **37,** 991–1003 (2004).

[20] R. Lappalainen and S. S. Santavirta, "Potential of coatings in total hip replacement," *Clin Orthop Relat Res* **430,** 72–9 (2005).

[21] R. Hauert, "A review of modified DLC coatings for biological applications," *Diam relat mater* **12,** 583–589 (2003).

[22] S. Lees, D. Hanson, E. Page, and H. A. Mook, "Comparison of dosage-dependent effects of beta-aminopropionitrile, sodium fluoride, and hydrocortisone on selected physical properties of cortical bone," *J Bone Miner Res* **9,** 1377–89 (1994).

[23] M. Yamauchi, E. P. Katz, K. Otsubo, K. Teraoka, and G. L. Mechanic, "Cross-linking and stereospecific structure of collagen in mineralized and nonmineralized skeletal tissues," *Connect Tissue Res* **21,** 159–67; discussion 168–9 (1989).

[24] D. Eyre, "New biomarkers of bone resorption," *J Clin Endocrinol Metab* **74,** 470A–470C (1992).

[25] A. L. Boskey, "Mineral-matrix interactions in bone and cartilage," *Clin Orthop Relat Res* **281,** 244–74 (1992).

[26] H. I. Roach, "Why does bone matrix contain non-collagenous proteins? The possible roles of osteocalcin, osteonectin, osteopontin and bone sialoprotein in bone mineralisation and resorption," *Cell Biol Int* **18,** 617–28 (1994).

[27] G. S. Keene, *Key topics in orthopaedic trauma surgery* (BIOS Scientific Publishers Ltd, Oxford, 1999).

[28] S. C. Manalagos and R. L. Jilka, "Bone marrow, cytokines, and bone remodelling: emerging insights into the pathophysiology of osteoporosis," *N Engl J Med* **332,** 305–311 (1995).

[29] S. Standring, ed., *Gray's anatomy: The Anatomical basis of clinical practice*, 40th ed. (Elsevier Churchill Livingstone, New York, 2005).

[30] C. V. Mow and W. C. Hayes, *Basic orthopaedic biomechanics* (Raven Press, New York, 1991).

[31] D. R. Carter, "Mechanical loading histories and cortical bone remodeling," *Calcif Tissue Int* **36 Suppl 1,** S19–24 (1984).

[32] D. R. Carter and W. C. Hayes, "Bone compressive strength: the influence of density and strain rate," *Science* **194,** 1174–6 (1976).

[33] T. A. Einhorn, *Biomechanics of Bone* (Academic Press, San Diego, CA, 1996).

[34] J. F. V. Vincent, *Structural biomaterials* (Macmillan Press, London, 1982).

[35] R. B. Martin and D. B. Burr, *Structure, function, and adaptation of compact bone* (Raven Press, New York, 1989).

[36] D. T. Reilly and A. H. Burstein, "The elastic and ultimate properties of compact bone tissue," *J Biomech* **8,** 393–405 (1975).

[37] S. A. Goldstein, "The mechanical properties of trabecular bone: dependence on anatomic location and function," *J Biomech* **20,** 1055–61 (1987).

[38] S. Cowin, *Bone mechanics* (CRC Press, Boca Raton, 1989).

[39] D. R. Carter, R. Vasu, and W. H. Harris, "The plated femur: relationships between the changes in bone stresses and bone loss," *Acta Orthop Scand* **52,** 241–8 (1981).

[40] J. D. Currey, "Mechanical properties of bone tissues with greatly differing functions," *J Biomech* **12,** 313–9 (1979).

[41] S. A. Wainwright, *Axis and circumference: the cylindrical shape of plants and animals* (Harvard University Press, Cambridge, 1988).

[42] S. Weiner and W. Traub, "Bone structure: from angstroms to microns," *FASEB J* **6,** 879–85 (1992).

[43] J. G. Skedros, M. W. Mason, M. C. Nelson, and R. D. Bloebaum, "Evidence of structural and material adaptation to specific strain features in cortical bone," *Anat Rec* **246,** 47–63 (1996).

[44] H. Oxlund, L. Mosekilde, and G. Ortoft, "Reduced concentration of collagen reducible cross links in human trabecular bone with respect to age and osteoporosis," *Bone* **19,** 479–84 (1996).

[45] C. T. Rubin, T. S. Gross, H. J. Donahue, F. Guilak, and K. J. McLeod, "Physical and environmental incluences on bone formation," in *Bone formation and repair*, C. Brighton and G. Friedlaender, eds. (American Academy of Orthopaedic Surgeons, Rosemont, 1994), pp. 61-78.

[46] L. Peltier, *Fractures: A history and iconography of their treatment* (Norman Publishing, San Francisco, 1990).

[47] M. E. Muller, J. M. Allgower, R. Schneiner, and H. Willenegger, *Manual of internal fixation*, 3 rd ed. (Springer-Verlag, Berlin, 1992).

[48] C. F. Brunner and B. G. Weber, *Special techniques in internal fixation* (Springer-Verlag, Berlin, 1982).

[49] A. K. Bhadra and C. S. Roberts, "Indications for antibiotic cement nails," *J Orthop Trauma* **23,** S26–30 (2009).

[50] B. D. Ratner, A. S. Hoffman, F. J. Schoen, and J. E. Lemons, *Biomaterials Science: An Introduction to Materials in Medicine*, Vol. 2, (Academic Press, New York, 1996).

[51] P. K. Chu, J. Y. Chen, L. P. Wang, and N. Huang, "Plasma-surface modification of biomaterials," *Mater Sci Eng R: Rep* **36,** 143–206 (2002).

[52] F. Pena, T. Grontvedt, G. A. Brown, A. K. Aune, and L. Engebretsen, "Comparison of failure strength between metallic and absorbable interference screws. Influence of insertion torque, tunnel-bone block gap, bone mineral density, and interference," *Am J Sports Med* **24,** 329–34 (1996).

[53] R. Lakatos, *General Principles of Internal Fixation* (WebMD, LLC, 2011).

[54] Z. H. You, W. H. Bell, E. D. Schneiderman, and R. B. Ashman, "Biomechanical properties of small bone screws," *J Oral Maxillofac Surg* **52,** 1293–302 (1994).

[55] C. R. Andrea, S. M. Stover, L. D. Galuppo, K. T. Taylor, and P. C. Rakestraw, "Comparison of insertion time and pullout strength between self-tapping and non-self-tapping AO 4.5-mm cortical bone screws in adult equine third metacarpal bone," *Vet Surg* **31,** 189–94 (2002).

[56] F. Baumgart, J. Cordey, K. Morikawa, S. M. Perren, B. Rahn, R. Schavan, and S. Snyder, "AO/ASIF self-tapping screws (STS)," *Injury* **24 (1.supplement),** 1–17 (1993).

[57] G. J. Bennett, *Materials and Materials Testing* (American Association of Neurological Surgeons, Park Ridge, IL, 1994).

[58] E. C. Benzel, *Implant-bone Interfaces* (McGraw-Hill, New York, 1995).

[59] Y. H. An and R. A. Draughn, *Mechanical testing of bone and the bone-implant interface* (CRC Press, Boca Raton, 2000).

[60] N. Ozkaya and M. Nordin, *Fundamentals of biomechanics*, 2.nd ed. (Springer-Verlag New York, Inc., New York, 1999).

[61] H. U. Cameron, *Bone implant interface* (Mosby-Year Book, Chicago, IL, 1994).

[62] R. Berkowitz, G. Njus, and G. Vrabec, "Pullout strength of self-tapping screws inserted to different depths," *J Orthop Trauma* **19,** 462–5 (2005).

[63] T. A. DeCoster, D. B. Heetderks, D. J. Downey, J. S. Ferries, and W. Jones, "Optimizing bone screw pullout force," *J Orthop Trauma* **4,** 169–74 (1990).

[64] J. R. Chapman, R. M. Harrington, K. M. Lee, P. A. Anderson, A. F. Tencer, and D. Kowalski, "Factors affecting the pullout strength of cancellous bone screws," *J Biomech Eng* **118,** 391–8 (1996).

[65] C. J. Ivanoff, L. Sennerby, C. Johansson, B. Rangert, and U. Lekholm, "Influence of implant diameters on the integration of screw implants. An experimental study in rabbits," *Int J Oral Maxillofac Surg* **26,** 141–8 (1997).

[66] C. Hallgren, H. Reimers, J. Gold, and A. Wennerberg, "The importance of surface texture for bone integration of screw shaped implants: an in vivo study of implants patterned by photolithography," *J Biomed Mater Res* **57,** 485–96 (2001).

[67] B. Sanden, C. Olerud, C. Johansson, and S. Larsson, "Improved bone-screw interface with hydroxyapatite coating: an in vivo study of loaded pedicle screws in sheep," *Spine* **26,** 2673–8 (2001).

[68] R. S. Squier, W. J. Psoter, and T. D. Taylor, "Removal torques of conical, tapered implant abutments: the effects of anodization and reduction of surface area," *Int J Oral Maxillofac Implants* **17,** 24–7 (2002).

[69] T. L. Bredbenner and R. H. Haug, "Substitutes for human cadaveric bone in maxillofacial rigid fixation research," *Oral Surg Oral Med Oral Pathol Oral Radiol Endod* **90,** 574–80 (2000).

[70] B. Orlando, A. Barone, T. M. Giorno, L. Giacomelli, P. Tonelli, and U. Covani, "Insertion Torque in Different Bone Models with Different Screw Pitch: An In Vitro Study," *Int J Oral & Maxillofac Implants* **25,** 883–887 (2010).

[71] K. J. Lawson and J. Brems, "Effect of insertion torque on bone screw pullout strength," *Orthopedics* **24,** 451–4 (2001).

[72] G. A. Brown, F. Pena, T. Grontvedt, D. Labadie, and L. Engebretsen, "Fixation strength of interference screw fixation in bovine, young

human, and elderly human cadaver knees: influence of insertion torque, tunnel-bone block gap, and interference," *Knee Surg Sports Traumatol Arthrosc* **3,** 238–44 (1996).

[73] B. Wilmes and D. Drescher, "Impact of bone quality, implant type, and implantation site preparation on insertion torques of mini-implants used for orthodontic anchorage," *Int J Oral Maxillofac Surg* **40,** 697–703 (2011).

[74] R. Brå nemark, L. O. Ohrnell, P. Nilsson, and P. Thomsen, "Biomechanical characterization of osseointegration during healing: An experimental in vivo study in the rat," *Biomaterials* **18,** 969–978 (1997).

[75] S. Raab, A. Ahmed, and J. Provan, "The quasistatic and fatique performance of the implant/bone cement interface," *J Biomed Mater Res* **15,** 159–181 (1981).

[76] M. T. Mantley, G. Kotzar, L. S. Stern, and A. Wilde, "Effects of Repetitive Loading on the Integrity of Porous Coatings," *Clin Orthop Relat Res* **217,** 293–302 (1987).

[77] B. R. Merk, S. H. Stern, S. Cordes, and E. P. Lautenschlager, "A fatigue life analysis of small fragment screws," *J Orthop Trauma* **15,** 494–9 (2001).

[78] A. Shirazi-Adl, M. Dammak, and D. J. Zukor, "Fixation pull-out response measurement of bone screws and porous-surfaced posts," *J biomech* **27,** 1249–58 (1994).

[79] T. H. Lim, H. S. An, T. Hasegawa, L. McGrady, K. Y. Hasanoglu, and C. R. Wilson, "Prediction of fatigue screw loosening in anterior spinal fixation using dual energy x-ray absorptiometry," *Spine* **20,** 2565–8; discussion 2569 (1995).

[80] R. L. Aper, A. S. Litsky, S. C. Roe, and K. A. Johnson, "Effect of bone diameter and eccentric loading on fatigue life of cortical screws used with interlocking nails," *Am J Vet Res* **64,** 569–73 (2003).

[81] S. M. Hou, J. L. Wang, and J. Lin, "Mechanical strength, fatigue life, and failure analysis of two prototypes and five conventional tibial locking screws," *J Orthop Trauma* **16,** 701–8 (2002).

[82] M. C. Thompson and D. S. Gesink, "Biomechanical comparison of syndesmosis fixation with 3.5- and 4.5-millimeter stainless steel screws," *Foot Ankle Int* **21,** 736–41 (2000).

[83] P. Bolind, C. B. Johansson, P. Johansson, G. Granstrom, and T. Albrektsson, "Retrieved implants from irradiated sites in humans: A histologic/histomorphometric investigation of oral and craniofacial implants," *Clin Implant Dent Relat Res* **8,** 142–150 (2006).

[84] D. Johnson, M. Tucci, R. McGuire, and J. Hughes, "Evaluation of the biomaterial-interface of screw threads in patients having clinical pain," *Biomed Sci Instrum* **32,** 127–33 (1996).

[85] J. H. Lee, J. H. Lee, J. W. Park, and Y. H. Shin, "The insertional torque of a pedicle screw has a positive correlation with bone mineral density in posterior lumbar pedicle screw fixation," *J Bone Joint Surg Br* **94,** 93–7 (2012).

[86] K. Okuyama, E. Abe, T. Suzuki, Y. Tamura, M. Chiba, and K. Sato, "Can insertional torque predict screw loosening and related failures? An in vivo study of pedicle screw fixation augmenting posterior lumbar interbody fusion," *Spine* **25,** 858–64 (2000).

[87] K. Okuyama, E. Abe, T. Suzuki, Y. Tamura, M. Chiba, and K. Sato, "Influence of bone mineral density on pedicle screw fixation: a study of pedicle screw fixation augmenting posterior lumbar interbody fusion in elderly patients," *Spine J* **1,** 402–7 (2001).

[88] G. Giavaresi, M. Fini, R. Chiesa, L. Rimondini, G. Rondelli, V. Borsari, L. Martini, N. Nicolialdini, G. A. Guzzardella, and R. Giardino, "Osseointegration of sandblasted or anodised hydrothermally-treated titanium implants: mechanical, histomorphometric and bone hardness measurements," *Int J Artif Organs* **25,** 806–13 (2002).

[89] G. Giavaresi, M. Fini, A. Cigada, R. Chiesa, G. Rondelli, L. Rimondini, P. Torricelli, N. N. Aldini, and R. Giardino, "Mechanical and histomorphometric evaluations of titanium implants with different surface treatments inserted in sheep cortical bone," *Biomaterials* **24,** 1583–94 (2003).

[90] J. Hyup Lee, H.-S. Ryu, D.-S. Lee, K. Sun Hong, B.-S. Chang, and C.-K. Lee, "Biomechanical and histomorphometric study on the bone-screw interface of bioactive ceramic-coated titanium screws," *Biomaterials* **26,** 3249–3257 (2005).

[91] S. Overgaard, M. Lind, H. Glerup, C. Bunger, and K. Soballe, "Porous-coated versus grit-blasted surface texture of

hydroxyapatite-coated implants during controlled micromotion: mechanical and histomorphometric results," *J Arthroplasty* **13,** 449–58 (1998).

[92] M. Rocca, M. Fini, G. Giavaresi, N. Nicoli Aldini, and R. Giardin, "Tibial implants: biomechanical and histomorphometric studies of hydroxyapatite-coated and uncoated stainless steel and titanium screws in long-term ovariectomized sheep," *Int J Artif Organs* **24,** 649–54 (2001).

[93] P. R. Klokkevold, R. D. Nishimura, M. Adachi, and A. Caputo, "Osseointegration enhanced by chemical etching of the titanium surface. A torque removal study in the rabbit," *Clin Oral Implants Res* **8,** 442–7 (1997).

[94] L. O. Ohrnell, R. Branemark, J. Nyman, P. Nilsson, and P. Thomsen, "Effects of irradiation on the biomechanics of osseointegration - An experimental in vivo study in rats," *Scand J Plast Reconstr Surg Hand Surg* **31,** 281–293 (1997).

[95] M. D. Rong, L. Zhou, Z. H. Gou, A. D. Zhu, and D. F. Zhou, "The early osseointegration of the laser-treated and acid-etched dental implants surface: an experimental study in rabbits," *J Mater Sci Mater Med* **20,** 1721–1728 (2009).

[96] M. Fini, G. Giavaresi, R. Giardino, F. Cavani, and R. Cadossi, "Histomorphometric and mechanical analysis of the hydroxyapatite-bone interface after electromagnetic stimulation: an experimental study in rabbits," *J Bone Joint Surg Br* **88,** 123–8 (2006).

[97] L. D. Galuppo, S. M. Stover, D. G. Jensen, and N. H. Willits, "A biomechanical comparison of headless tapered variable pitch and AO cortical bone screws for fixation of a simulated lateral condylar fracture in equine third metacarpal bones," *Vet Surg* **30,** 332–40 (2001).

[98] C. Rahm, K. Ito, and J. Auer, "Screw fixation in lag fashion of equine cadaveric metacarpal and metatarsal condylar bone specimens: a biomechanical comparison of shaft and cortex screws," *Vet Surg* **29,** 564–71 (2000).

[99] L. D. Galuppo, S. M. Stover, and D. G. Jensen, "A biomechanical comparison of equine third metacarpal condylar bone fragment compression and screw pushout strength between headless tapered

variable pitch and AO cortical bone screws," *Vet Surg* **31,** 201–10 (2002).

[100] T. A. Zdeblick, D. N. Kunz, M. E. Cooke, and R. McCabe, "Pedicle screw pullout strength. Correlation with insertional torque," *Spine* **18,** 1673–6 (1993).

[101] N. E. Motzkin, E. Y. Chao, K. N. An, M. A. Wikenheiser, and D. G. Lewallen, "Pull-out strength of screws from polymethylmethacrylate cement," *J Bone Joint Surg Br* **76,** 320–3 (1994).

[102] T. Pitzen, F. Franta, D. Barbier, and W. I. Steudel, "Insertion torque and pullout force of rescue screws for anterior cervical plate fixation in a fatigued initial pilot hole," *J Neurosurg Spine* **1,** 198–201 (2004).

[103] L. Ballerini, V. Franke-Stenport, G. Borgefors, and C. B. Johansson, "Comparison of histomorphometrical data obtained with two different image analysis methods," *J Mater Sci Mater Med* **18,** 1471–1479 (2007).

[104] P. Bolind, C. B. Johansson, T. J. Balshi, B. Langer, and T. Albrektsson, "A study of 275 retrieved Branemark oral implants," *Int J Periodontics Restorative Dent* **25,** 425–437 (2005).

[105] C. J. Ivanoff, G. Widmark, C. Johansson, and A. Wennerberg, "Histologic evaluation of bone response to oxidized and turned titanium micro-implants in human jawbone," *Int J Oral Maxillofac Implants* **18,** 341–8 (2003).

[106] Y. T. Sul, C. Johansson, E. Byon, and T. Albrektsson, "The bone response of oxidized bioactive and non-bioactive titanium implants," *Biomaterials* **26,** 6720–30 (2005).

[107] Y. T. Sul, C. B. Johansson, K. Roser, and T. Albrektsson, "Qualitative and quantitative observations of bone tissue reactions to anodised implants," *Biomaterials* **23,** 1809–17 (2002).

[108] B. Kincaid, L. Schroder, and J. Mason, "Measurement of orthopedic cortical bone screw insertion performance in cadaver bone and model materials," *Exp Mech* **47,** 595–607 (2007).

[109] C. A. Reitman, L. Nguyen, and G. R. Fogel, "Biomechanical evaluation of relationship of screw pullout strength, insertional torque, and bone mineral density in the cervical spine," *J Spinal Disord Tech* **17,** 306–11 (2004).

[110] C. R. Glauser, Z. M. Oden, C. G. Ambrose, M. B. Willits, and K. J. Coupe, "Mechanical testing of small fracture implants for comparison of insertion and failure torques," *Arch Orthop Trauma Surg* **123,** 388–91 (2003).

[111] T. C. Lee, S. Mohsin, D. Taylor, R. Parkesh, T. Gunnlaugsson, F. J. O'Brien, M. Giehl, and W. Gowin, "Detecting microdamage in bone," *J Anat* **203,** 161–72 (2003).

[112] H. M. Frost, "Metabolism of bone," *N Engl J Med* **289,** 864–5 (1973).

[113] D. B. Burr, T. Yoshikawa, D. Teegarden, R. Lyle, G. McCabe, L. D. McCabe, and C. M. Weaver, "Exercise and oral contraceptive use suppress the normal age-related increase in bone mass and strength of the femoral neck in women 18-31 years of age," *Bone* **27,** 855–63 (2000).

[114] S. Mori and D. B. Burr, "Increased intracortical remodeling following fatigue damage," *Bone* **14,** 103–9 (1993).

[115] V. Bentolila, T. M. Boyce, D. P. Fyhrie, R. Drumb, T. M. Skerry, and M. B. Schaffler, "Intracortical remodeling in adult rat long bones after fatigue loading," *Bone* **23,** 275–81 (1998).

[116] O. Verborgt, G. J. Gibson, and M. B. Schaffler, "Loss of osteocyte integrity in association with microdamage and bone remodeling after fatigue in vivo," *J Bone Miner Res* **15,** 60–7 (2000).

[117] B. Martin, "Aging and Strength of Bone as a Structural Material," *Calcif Tissue Int* **53,** S34–S40 (1993).

[118] D. T. Reilly and A. H. Burstein, "Review article. The mechanical properties of cortical bone," *J Bone Joint Surg Am* **56,** 1001–22 (1974).

[119] P. Augat and S. Schorlemmer, "The role of cortical bone and its microstructure in bone strength," *Age and Ageing* **35,** 27–31 (2006).

[120] D. E. Steflik, R. S. Corpe, T. R. Young, G. R. Parr, M. Tucker, M. Sims, J. Tinley, A. Sisk, and M. McDaniel, "Light microscopic and scanning electron microscopic retrieval analyses of implanted biomaterials retrieved from humans and experimental animals," *J Oral Implantol* **27,** 5–15 (2001).

[121] D. R. Carter and W. C. Hayes, "Compact bone fatigue damage: a microscopic examination," *Clin Orthop Relat Res* **127,** 265–74 (1977).

[122] P. Zioupos, J. D. Currey, and A. J. Sedman, "An examination of the micromechanics of failure of bone and antler by acoustic emission tests and Laser Scanning Confocal Microscopy," *Med Eng Phys* **16,** 203–12 (1994).

[123] J. A. Timlin, A. Carden, M. D. Morris, R. M. Rajachar, and D. H. Kohn, "Raman spectroscopic imaging markers for fatigue-related microdamage in bovine bone," *Anal Chem* **72,** 2229–36 (2000).

[124] H. Ikeda, P. E. Rossouw, P. M. Campbell, E. Kontogirogos, and P. H. Buschang, "Three-dimensional analysis of peri-boneimplant contact of rough-surface miniscrew implants," *American Journal of Orthodontics and Dentofacial Orthopedics* **139,** e153–e163 (2011).

[125] H. Sarve, B. Friberg, G. Borgefors, and C. B. Johansson, "Introducing a Novel Analysis Technique for Osseointegrated Dental Implants Retrieved 29 Years Postsurgery," *Clinical Implant Dentistry and Related Research* (2011).

[126] H. Sarve, J. Lindblad, G. Borgefors, and C. B. Johansson, "Extracting 3D information on bone remodeling in the proximity of titanium implants in SRCT image volumes," *Computer Methods and Programs in Biomedicine* **102,** 25–34 (2011).

[127] W. Heidemann, K. L. Gerlach, K. H. Grobel, and H. G. Kollner, "Influence of different pilot hole sizes on torque measurements and pullout analysis of osteosynthesis screws," *J Craniomaxillofac Surg* **26,** 50–5 (1998).

[128] S. Inceoglu, A. Akbay, and R. F. McLain, "Stress relaxation at the bone-pedicle screw interface in human bone," *Spine* **31,** 1321–6 (2006).

[129] A. Moroni, C. Faldini, M. Rocca, S. Stea, and S. Giannini, "Improvement of the bone-screw interface strength with hydroxyapatite-coated and titanium-coated AO/ASIF cortical screws," *J Orthop Trauma* **16,** 257–63 (2002).

[130] S. Aisenberg and R. Chabot, "Ion Beam Deposition of Thin Films of Diamondlike Carbon," *Journal of Applied Physics* **42,** 2953–2958 (1971).

[131] R. Lappalainen, A. Anttila, and H. Heinonen, "Diamond coated total hip replacements," *Clin Orthop* 118-27 (1998).

[132] V.-M. Tiainen, "Amorphous carbon as a bio-mechanical coating - mechanical properties and biological applications," *Diam relat mater* **10,** 153–160 (2001).

[133] A. Grill, "Diamond-like carbon coatings as biocompatible materials–an overview," *Diam relat mater* **12,** 166–170 (2003).

[134] J. Robertson, "Diamond-like amorphous carbon," *Materials Science and Engineering: R: Reports* **37,** 129–281 (2002).

[135] A. Anttila, J.-P. Hirvonen, and J. Koskinen, "Procedure and apparatus for the coating of materials by means of a pulsating plasma beam," *US Patent 5078848* (1992).

[136] D. McKenzie, "Tetrahedral Bonding in Amorphous Carbon," *Reports in Progress in Physics* **59,** 1611–1664 (1996).

[137] Y. Lifshitz, "Diamond-like Carbon - Present Status," *Diam relat mater* **8,** 1659–1676 (1999).

[138] D. McKenzie, D. Muller, and B. Pailthorpe, "Compressive-stress-induced formation of thin-film tetrahedral amorphous carbon," *Physical Review Letters* **67,** 773–776 (1991).

[139] A. Anttila, R. Lappalainen, M. Hakovirta, and J. Salo, "Improvement of adhesion of diamond-like coatings using whisker-composite techniques," *Surface and Coatings Technology* **82,** 130–132 (1996).

[140] M. Hakovirta, J. Salo, A. Anttila, and R. Lappalainen, "Graphite particles in the diamond-like a-C films prepared with the pulsed arc-discharge method," *Diam relat mater* **4,** 1335–1339 (1995).

[141] S. Santavirta, Y. T. Konttinen, R. Lappalainen, A. Anttila, S. B. Goodman, M. Lind, L. Smith, M. Takagi, E. Gomez-Barrena, L. Nordsletten, and J. W. Xu, "Materials in total joint replacement," *Current Orthopaedics* **12,** 51–57 (1998).

[142] S. S. Santavirta, R. Lappalainen, P. Pekko, A. Anttila, and Y. T. Konttinen, "The counterface, surface smoothness, tolerances, and coatings in total joint prostheses," *Clin Orthop Rela Res* 92-102 (1999).

[143] R. Hauert, "DLC Films in Biomedical Applications," in *Tribology of Diamond-like Carbon Films: Fundamentals and Applications*, C. Donnet and A. Erdemir, eds. (Springer, New York, 2008), pp. 494-509.

[144] D. Sheeja, B. K. Tay, X. Shi, S. P. Lau, C. Daniel, S. M. Krishnan, and L. N. Nung, "Mechanical and tribological characterization of diamond-like carbon coatings on orthopaedic materials," *Diam relat mater* **10,** 1043–1048 (2001).

[145] A. A. Voevodin and M. S. Donley, "Preparation of amorphous diamond-like carbon by pulsed laser deposition: a critical review," *Surface & Coatings Technology* **82,** 199–213 (1996).

[146] D. P. Dowling, P. V. Kola, K. Donnelly, T. C. Kelly, K. Brumitt, L. Lloyd, R. Eloy, M. Therin, and N. Weill, "Evaluation of diamond-like carbon-coated orthopaedic implants," *Diam relat mater* **6,** 390–393 (1997).

[147] R. Lappalainen, V. Myllymaki, L. Pulli, and J. Makitalo, "Method for Producing High-Quality Surfaces and a Product Having a High-Quality Surface," *US Patent 20090169871* (2009).

[148] S. Myllymaa, K. Myllymaa, and R. Lappalainen, "Flexible Implantable Thin Film Electrodes," in *Recent Advances in Biomedical Engineering*, N. R. Naik, ed. (In-Tech, Vukovar, 2009), pp. 165-189.

[149] G. A. Brown, T. McCarthy, C. A. Bourgeault, and D. J. Callahan, "Mechanical performance of standard and cannulated 4.0-mm cancellous bone screws," *J Orthop Res* **18,** 307–12 (2000).

[150] K. J. Faran, N. Ichioka, M. A. Trzeciak, S. Han, J. Medige, and O. J. Moy, "Effect of bone quality on the forces generated by compression screws," *J Biomech* **32,** 861–64 (1999).

[151] C. C. Hsu, C. K. Chao, J. L. Wang, S. M. Hou, Y. T. Tsai, and J. Lin, "Increase of pullout strength of spinal pedicle screws with conical core: biomechanical tests and finite element analyses," *J Orthop Res* **23,** 788–94 (2005).

[152] S. Battula, A. Schoenfeld, G. Vrabec, and G. O. Njus, "Experimental evaluation of the holding power/stiffness of the self-tapping bone screws in normal and osteoporotic bone material," *Clin Biomech (Bristol, Avon)* **21,** 533–7 (2006).

[153] W. D. j. Callister, *Materials science and engineering. An introduction*, 5 th ed. (John Wiley & Sons, Inc., New York, 2000).

[154] Opetushallitus, *Puuteollisuus* (Opetushallitus, 2003).

[155] I. A. Karnezis, A. W. Miles, J. L. Cunningham, and I. D. Learmonth, "Axial preload in external fixator half-pins: a preliminary mechanical study of an experimental bone anchorage system," *Clin Biomech (Bristol, Avon)* **14,** 69–73 (1999).

[156] C. R. Russo, F. Lauretani, S. Bandinelli, B. Bartali, A. Di Iorio, S. Volpato, J. M. Guralnik, T. Harris, and L. Ferrucci, "Aging bone in men and women: beyond changes in bone mineral density," *Osteoporos int* **14,** 531–8 (2003).

[157] J. Rittweger, G. Beller, J. Ehrig, C. Jung, U. Koch, J. Ramolla, F. Schmidt, D. Newitt, S. Majumdar, H. Schiessl, and D. Felsenberg, "Bone-muscle strength indices for the human lower leg," *Bone* **27,** 319–26 (2000).

[158] D. Meleo, L. Baggi, M. Di Girolamo, F. Di Carlo, R. Pecci, and R. Bedini, "Fixture-abutment connection surface and micro-gap measurements by 3D micro-tomographic technique analysis," *Annali dell'Istituto superiore di sanita* **48,** 53–8 (2012).

[159] D. Meleo, R. Bedini, R. Pecci, F. Mangione, and L. Pacifici, "Microtomographic and morphometric characterization of a bioceramic bone substitute in dental implantology," *Annali dell'Istituto superiore di sanita* **48,** 59–64 (2012).

[160] S. Mitura, P. Niedzielski, D. Jachowicz, M. Langer, J. Marciniak, A. Stanishevsky, E. Tochitsky, P. Louda, P. Couvrat, M. Denis, and P. Lourdin, "Influence of carbon coatings origin on the properties important for biomedical application," *Diam Rel Mater* **5,** 1185–1188 (1996).

[161] M. A. Wikenheiser, M. D. Markel, D. G. Lewallen, and E. Y. Chao, "Thermal response and torque resistance of five cortical half-pins under simulated insertion technique," *J Orthop Res* **13,** 615–9 (1995).

[162] J. Toyras, R. K. Korhonen, T. Voutilainen, J. S. Jurvelin, and R. Lappalainen, "Improvement of arthroscopic cartilage stiffness probe using amorphous diamond coating," *J Biomed Mater Res B Appl Biomater* **73,** 15–22 (2005).

[163] J. J. Jaatinen, R. K. Korhonen, A. Pelttari, H. J. Helminen, H. Korhonen, R. Lappalainen, and H. Kroger, "Early bone growth on the surface of titanium implants in rat femur is enhanced by an amorphous diamond coating," *Acta Orthop* **82,** 499–503 (2011).

[164] A. H. Burstein, J. Currey, V. H. Frankel, K. G. Heiple, P. Lunseth, and J. C. Vessely, "Bone strength. The effect of screw holes," *J Bone Joint Surg Am* **54,** 1143–56 (1972).

[165] A. Trampuz and W. Zimmerli, "Diagnosis and treatment of infections associated with fracture-fixation devices," *Injury* **37,** 59–66 (2006).

[166] D. J. Hak and M. McElvany, "Removal of broken hardware," *J Am Acad Orthop Surg* **16,** 113–120 (2008).

[167] R. B. Minkowitz, S. Bhadsavle, M. Walsh, and K. A. Egol, "Removal of painful orthopaedic implants after fracture union," *J bone joint surg Am* **89A,** 1906–1912 (2007).

[168] T. M. Cleek, K. J. Reynolds, and T. C. Hearn, "Effect of screw torque level on cortical bone pullout strength," *J Orthop Trauma* **21,** 117–23 (2007).

[169] P. Bolind, C. Acton, T. Albrektsson, P. Bonding, G. Granstrom, C. Johansson, P. Lindeman, W. Muhlbauer, and A. Tjellstrom, "Histologic evaluation of retrieved craniofacial implants," *Otolaryngol head neck Surg* **123,** 140–146 (2000).

[170] H. Sievanen, P. Kannus, V. Nieminen, A. Heinonen, P. Oja, and I. Vuori, "Estimation of various mechanical characteristics of human bones using dual energy X-ray absorptiometry: methodology and precision," *Bone* **18,** 17S–27S (1996).

[171] N. J. Wachter, G. D. Krischak, M. Mentzel, M. R. Sarkar, T. Ebinger, L. Kinzl, L. Claes, and P. Augat, "Correlation of bone mineral density with strength and microstructural parameters of cortical bone in vitro," *Bone* **31,** 90–5 (2002).

[172] L. Duchemin, V. Bousson, C. Raossanaly, C. Bergot, J. D. Laredo, W. Skalli, and D. Mitton, "Prediction of mechanical properties of cortical bone by quantitative computed tomography," *Med Eng Phys* **30,** 321–8 (2008).

[173] T. Mikkola, S. Sipila, E. Portegijs, M. Kallinen, M. Alen, I. Kiviranta, M. Pekkonen, and A. Heinonen, "Impaired geometric properties of tibia in older women with hip fracture history," *Osteoporos Int* **18,** 1083–1090 (2007).

Original publications

Paper I

Apparatus to test insertion and removal torque of bone screws

Koistinen A., Santavirta S.S. and Lappalainen R.

Proceedings of the Institution of Mechanical Engineers, Part H: Journal of Engineering in Medicine, **217**, 503–508, 2003

Paper **II**

Effect of bone mineral density and amorphous diamond coatings on insertion torque of bone screws

Koistinen A., Santavirta S.S., Kröger H. and Lappalainen R.

Biomaterials, **26**, 5687–5694, 2005

Paper **III**

Analysis of plastic deformation in cortical bone after insertion of coated and non-coated self-tapping orthopaedic screws

Koistinen A.P., Korhonen H., Kiviranta I., Kröger H. and Lappalainen R.

Proceedings of the Institution of Mechanical Engineers, Part H: Journal of Engineering in Medicine, **225**, 629–639, 2011

Paper **IV**

Interfacial sliding properties of bone screw materials and their effect on screw fixation strength

Koistinen A.P., Korhonen H., Kröger H. and Lappalainen R.

submitted for publication in Journal of Applied Biomaterials & Functional Materials

Arto Koistinen

Improvement of Orthopaedic Bone Screws by DLC Coatings

In Vitro Methods for Testing of Screw Fixation

Bone screws are the most common implants in orthopaedics and dentistry. However, corroded surfaces can complicate late removal of the screws and lead to failure of a screw or bone. In this thesis, performance of biocompatible diamond-like carbon (DLC) coating was studied on fracture fixation screws with in vitro mechanical tests. DLC coating resulted in at maximum 50 % lower insertion torque. Fixation strength of the screws was dependent on the mechanical properties of the test blocks, such as bone mineral density or elastic modulus of the material. The results suggest possible clinical application of DLC inducing improvement of bone-implant interaction and tribological features of bone screws.

UNIVERSITY OF EASTERN FINLAND

Publications of the University of Eastern Finland

Dissertations in Forestry and Natural Sciences

ISBN 978-952-61-0949-7